

NO-0210 002

APPLICATION OF A BEND-FIELD ENTER QUALITY MODEL (U)  
TULANE UNIV NEW ORLEANS LA DEPT OF CIVIL ENGINEERING  
B A BENEDICT JUL 79 AFOSR-TR-89-1410 AFOSR-77-1302

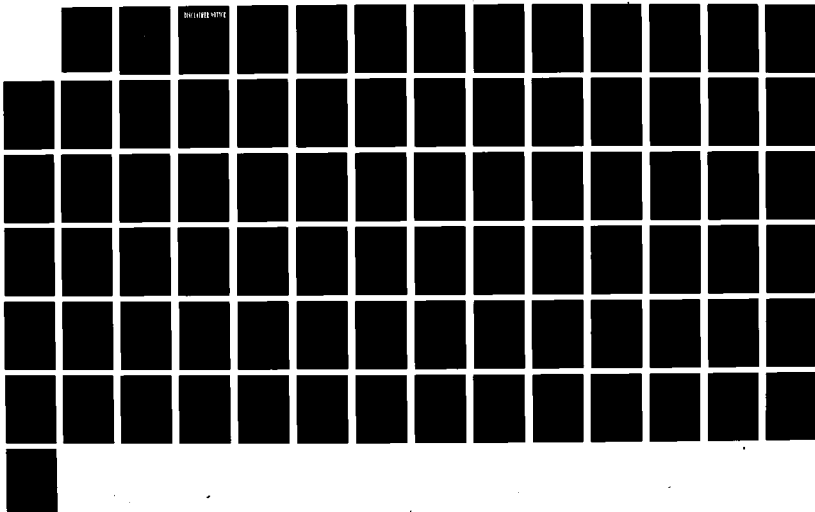
1/1

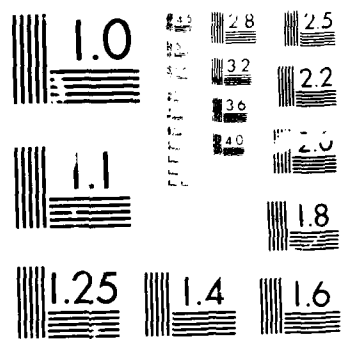
UNCLASSIFIED

F/B 24/4

NL

NO-0210 002





AD-A214 862

## REPORT DOCUMENTATION PAGE

Form Approved  
OMB No. 0704-0188

Public reporting burden for this collection of information is estimated to average 1 hour per response, including the time for reviewing instructions, searching existing data sources, gathering and maintaining the data needed, and completing and reviewing the collection of information. Send comments regarding this burden estimate or any other aspect of this collection of information, including suggestions for reducing this burden, to Washington Headquarters Services, Directorate for Information Operations and Reports, 1215 Jefferson Davis Highway, Suite 1204, Arlington, VA 22202-4302, and to the Office of Management and Budget, Paperwork Reduction Project (0704-0188), Washington, DC 20503.

1. AGENCY USE ONLY (Leave blank)		2. REPORT DATE July 1979	3. REPORT TYPE AND DATES COVERED Final/ 01 April-31 Mar 78	
4. TITLE AND SUBTITLE APPLICATION OF A NEAR-FIELD WATER QUALITY MODEL			5. FUNDING NUMBERS  61102F 2312/D9	
6. AUTHOR(S) Barry A. Benedict				
7. PERFORMING ORGANIZATION NAME(S) AND ADDRESS(ES) Tulane University Department of Civil Engineering New orleans, Lousiana 70118			8. PERFORMING ORGANIZATION REPORT NUMBER	
9. SPONSORING/MONITORING AGENCY NAME(S) AND ADDRESS(ES) AFOSR BLDG 410 BAFB DC 20332-6448			10. SPONSORING/MONITORING AGENCY REPORT NUMBER  AFOSR 77- 3302	
11. SUPPLEMENTARY NOTES				
12a. DISTRIBUTION/AVAILABILITY STATEMENT  Approved distribution			12b. DISTRIBUTION CODE	
13. ABSTRACT (Maximum 200 words) A two-dimensional near-field water quality model has been developed to describe the behavior of effluents dominated by jet mixing. Verification against data is good and demonstrates the model's utility and reliability. It can be employed as a planning and assessment tool for water quality studies. The model provides the ability to assess localized impacts in excess of that shown by the usual one-dimensional models. The primary limitations of the model are: 1) the model is invalid for cases where vertical mixing is significant; 2) the model does not deal well with highly bouyant discharges; 3) the model does not account for the existence of solid boundaries; 4) the model may become invalid before the one-dimensional region is reached, requiring the use of a diffusion model to carry the calculations further downstream.				
14. SUBJECT TERMS			15. NUMBER OF PAGES 79	
			16. PRICE CODE	
17. SECURITY CLASSIFICATION OF REPORT unclassified	18. SECURITY CLASSIFICATION OF THIS PAGE unclassified	19. SECURITY CLASSIFICATION OF ABSTRACT	20. LIMITATION OF ABSTRACT	

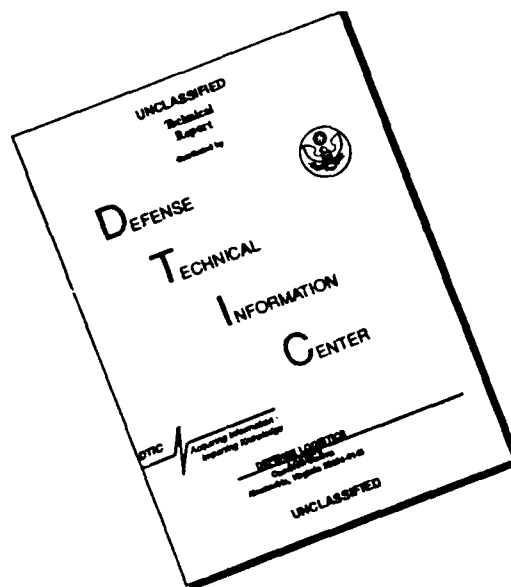
NSN 7540-01-280-5500

Standard Form 298 (890104 Draft)  
Prescribed by ANSI Std. Z39-18  
298-01

02 11

096

# DISCLAIMER NOTICE



THIS DOCUMENT IS BEST QUALITY AVAILABLE. THE COPY FURNISHED TO DTIC CONTAINED A SIGNIFICANT NUMBER OF PAGES WHICH DO NOT REPRODUCE LEGIBLY.

APPLIATION OF A NEAR-FIELD  
WATER QUALITY MODEL

by

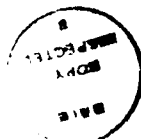
Barry A. Benedict  
Department of Civil Engineering  
Tulane University  
New Orleans, Louisiana 70118

FINAL REPORT FOR MINIGRANT AFOSR 77-3302

Air Force Office of Scientific Research  
Air Force Systems Command  
Bolling Air Force Base, D.C. 20332

## TABLE OF CONTENTS

SECTION I - INTRODUCTION AND PREVIOUS STATUS	1
INTRODUCTION	1
PREVIOUS WORK	1
DEVELOPMENT OF A NEAR-FIELD MODEL	2
MODEL APPROACH AND ASSUMPTIONS	3
EQUATION DEVELOPMENT	6
SOLUTION OF MODEL EQUATIONS	8
PRELIMINARY RESULTS AND ONGOING WORK	8
RESEARCH OBJECTIVES	8
SECTION II - BOUNDARY INFLUENCES	10
PROBLEM IDENTIFICATION	10
INTERFERENCE BY NEAR BANK	10
INTERFERENCE BY FAR BANK	16
OTHER METHODS FOR APPROXIMATION OF BOUNDARY INFLUENCES	17
USE OF IMAGE SOURCES	17
SCHEMATIZATION OF DISCHARGE	18
LINKAGE OF JET AND DIFFUSION MODELS	19
SUMMARY OF APPROACHES AND LIMITATIONS	22
SECTION III - ZONE OF FLOW ESTABLISHMENT BASIC BEHAVIOR	24
ZOFE TREATMENT IN CURRENT MODEL	25
IMPROVEMENTS IN CURRENT DESCRIPTION	26
RECOMMENDATIONS FOR ZOFE	27
SECTION IV - INCLUSION OF OTHER PARAMETERS	28
GENERAL MODELING	28
INCLUSION OF BOD SETTLING	28



<b>Accession For</b>	
NTIS GRA&I	<input checked="" type="checkbox"/>
DTIC TAB	<input type="checkbox"/>
Unannounced	<input type="checkbox"/>
Justification	
By	
Distribution/	
<b>Availability Codes</b>	
Dist	Avail and/or Special
A-1	

SECTION V - DEFINITION OF END OF JET REGION	30
LIMITATIONS TO JET MODEL	30
PREVIOUS DEFINITIONS OF JET ENDING	30
RELATIONSHIP OF ENTRAINMENT TO SPREADING	30
SPREADING RATIO IN DIFFUSION SOLUTIONS	32
STATUS OF FINDINGS ON END OF JET REGION	39
SECTION VI - VERIFICATION AND SENSITIVITY	40
GENERAL	40
SENSITIVITY	40
ENTRAINMENT COEFFICIENT	41
DRAG COEFFICIENT, $C_d$	42
ANGLE AT END OF ZONE, $\beta_0$	42
AMBIENT BOD, $L_a$	44
SEDIMENTATION COEFFICIENT, $K_3$	44
REVIEW OF SENSITIVITY FINDINGS	44
VERIFICATION	45
CENTERLINE TEMPERATURE DECREASE	46
LATERAL VARIATION OF CONSTITUENTS	46
VARIATION OF PLUME WIDTH	49
GENERAL ON VERIFICATION	49
EXAMPLE OF MODEL UTILITY	49
SECTION VII - SUMMARY OF FINDINGS AND RECOMMENDED WORK	52
APPLICABILITY OF MODEL	52
RECOMMENDED WORK	52
EXTENSION TO THREE DIMENSIONS	52
INCLUSION OF BOUNDARY EFFECTS	53
SOURCES AND SINKS	55
NON-UNIFORM SYSTEMS	55
CONCLUSIONS	56
REFERENCES	57
APPENDIX	61

# LIST OF TABLES

<u>TABLE</u>	<u>TITLE</u>	<u>PAGE</u>
1	VALUES OF CUTOFF VELOCITY RATIO FOR EXAMPLE	38
2	ADDED GUIDELINES FOR DEFINING END OF JET REGION	38
3	PARAMETER VALUES FOR BASIC CASE	40
4	SOME RESULTS OF VARYING THE ENTRAINMENT COEFFICIENT	41
5	RESULTS OF VARYING OTHER COEFFICIENT	42
6	GENERAL PLUME CHARACTERISTICS FOR VARIATION OF INITIAL ANGLE	43
7	DILUTION COMPARISONS FOR VARIATION OF INITIAL ANGLE ( $E = 0.05$ )	43
8	DATA FROM TWO-DIMENSIONAL RUNS BY CARTER, ET AL (16)	45



## LIST OF FIGURES

<u>FIGURE</u>	<u>PAGE</u>
1. SCHEMATIC OF JET PROBLEM	4
2. NEAR SHORE BEHAVIOR	11
3. WALL JET BEHAVIOR	14
4. SPREADING RATIO FROM JET MODEL	37
5. CENTERLINE TEMPERATURE DECREASE	47
6. LATERAL VARIATION OF CONCENTRATION	43
7. EFFECT OF DISCHARGE MODE ON BOD	50

## SECTION I

### INTRODUCTION AND PREVIOUS STATUS

A model to describe near-field distribution of water quality parameters was developed by the author in the summer of 1976 under an AFOSR program at Tyndall Air Force Base. This report details further developments and recommended research with this model. In addition, its utility is demonstrated. Section I is intended to briefly review the original model findings, outlined in detail in a report by Benedict (1).

### INTRODUCTION

It is standard practice to employ a one-dimensional analysis to study many water quality parameters, such as the dissolved oxygen (DO) and biochemical demand (BOD) pair. Use of the one-dimensional approach assumes that the quantities of interest are fully mixed both laterally and vertically across the stream from the point of discharge.

The discharge configuration most likely to achieve this early mixing is a submerged diffuser extending across the full stream width. Many discharges occur from the pipes or canals at the stream bank, however. It is believed that in some cases the one-dimensional (1-D) approach may not then be adequate and regions of the receiving water body might be subjected to greater stress (e.g., higher BOD and lower DO) than indicated by the 1-D analysis. For this reason, the work described here is underway, with the goal of providing an assessment and planning tool which enables projection of water quality conditions in the near-field, with an ability to determine the sensitivity of the receiving stream to the discharge configuration.

### PREVIOUS WORK

The model in its initial form deals only with DO and BOD, but it will be seen that subsequently other parameters could easily be added. The standard, simple first-order reactions for these parameters are shown in Equations 1 and 2 and used here.

$$\frac{dL}{dt} = K_1 L \quad (1)$$

$$\frac{dD}{dt} = K_1 L - K_2 D \quad (2)$$

in which

L = BOD in mg/l  
D = DO deficit in mg/l  
=  $C_s - C$   
C = actual DO in concentration  
 $C_s$  = saturation DO concentration of the water at the  
same temperature and pressure  
 $K_1$  = deoxygenation coefficient, units time<sup>-1</sup>  
 $K_2$  = reaeration coefficient, units time<sup>-1</sup>  
t = time

These equations quite obviously do not include all the sources and sinks of BOD and DO. Sedimentation, benthic demand, photosynthesis, dispersion, and two-stage BOD decay are among the factors which may be important in a given case. Initially only the  $K_1$  and  $K_2$  terms will be included to gain a feeling for system behavior, but it will be seen that addition of the other terms to the model will present no problem.

Solutions exist to these equations for a number of cases. Of interest here is the one-dimensional, steady-state, continuous discharge of a BOD load. The reader is referred to works such as Dobbins (2), Velz (3) and Nemerow (4) for these solutions. Later reference to 1-D solutions in this paper will mean these solutions.

Work by Holley, et al (5), Ward (6), and others enable one to estimate the downstream distance required for a discharge to fully mix laterally with the stream. This distance can sometimes be very great, especially where the stream width is large compared to the discharge structure dimension, making the use of the one-dimensional model suspect in those cases.

Rood and Holley (7) have drawn on diffusion equation solutions to study the effect of transverse mixing on the DO-BOD problem. As noted many places, e.g., Benedict, et al (8), such solutions show effects of ambient turbulence, but neglect the influence of jet action on initial mixing. Their results are extremely useful, however, in clearly illustrating the inadequacy of the 1-D approach in some cases. It may be, however, that the neglect of initial mixing may cause overestimation of impact.

#### DEVELOPMENT OF A NEAR-FIELD MODEL

The model to be shown here is a simpler first version of the ultimate model. Simplifications have been made in order to study the impact of near-field mixing on the DO-BOD problem in an uncomplicated way. As better understanding is gained, additional elements can be added to the model. The work done in recent years on the dynamics of heated water discharges will form the basis for the approach to be used here. Benedict, et al (9) and Jirka, et al (10) present summaries of these earlier efforts.

The discharge to be modeled is a non-buoyant canal discharge entering the receiving stream at its side. The discharge is assumed two-dimensional in that it is fully mixed vertically as might occur in a shallow stream. Figure 1 shows a schematic view of the problem.

#### MODEL APPROACH AND ASSUMPTIONS

The model to be developed here is an integral type. Mathematical forms are selected for the lateral variation of important properties about the jet (or discharge plume) axis. These profile forms are then integrated within the basic conservation equations. This integration reduces the problem to a one-dimensional one and simplifies numerical solution considerably.

The mathematical form of the lateral profiles remains the same along the jet axis, and these profiles are therefore called similar profiles. Morton (11) points out that the effect of assuming similar profiles and the form of the inflow velocity is to suppress analytic solution of the details of the lateral structure of the jet. Therefore, any reasonable profile shape can be assumed (e.g., a Gaussian curve) although all evidence implies that some sort of bell shape is more descriptive of the lateral profile than, say, a top-hat profile (values constant across plume). The forms chosen for this model are polynomials originally proposed by Abramovich (12) and used in a heated discharge model by Stolzenbach and Harleman (13). They are given in the following equations and schematically indicated in Figure 1.

$$u = U_a \cos \beta + u_c f(\eta/b) \quad (3)$$

$$f(\eta/b) = \left\{ 1 - [\eta/b]^2 \right\}^2 \quad (4)$$

$$L = L_a + L_c g(\eta, b) \quad (5)$$

$$D_a = D_c + D g(\eta, b) \quad (6)$$

$$g(\eta, b) = f(\eta/b) = 1 - (\eta/b)^2 \quad (7)$$

in which  $L_a$  = ambient BOD

$D_a$  = ambient DO deficit

$u$  = velocity in jet

$u_c$  = centerline excess velocity in jet

$\eta$  = lateral distance in jet measured from axis ( $\eta=0$ )  
and normal to the axis

$b$  = jet half width

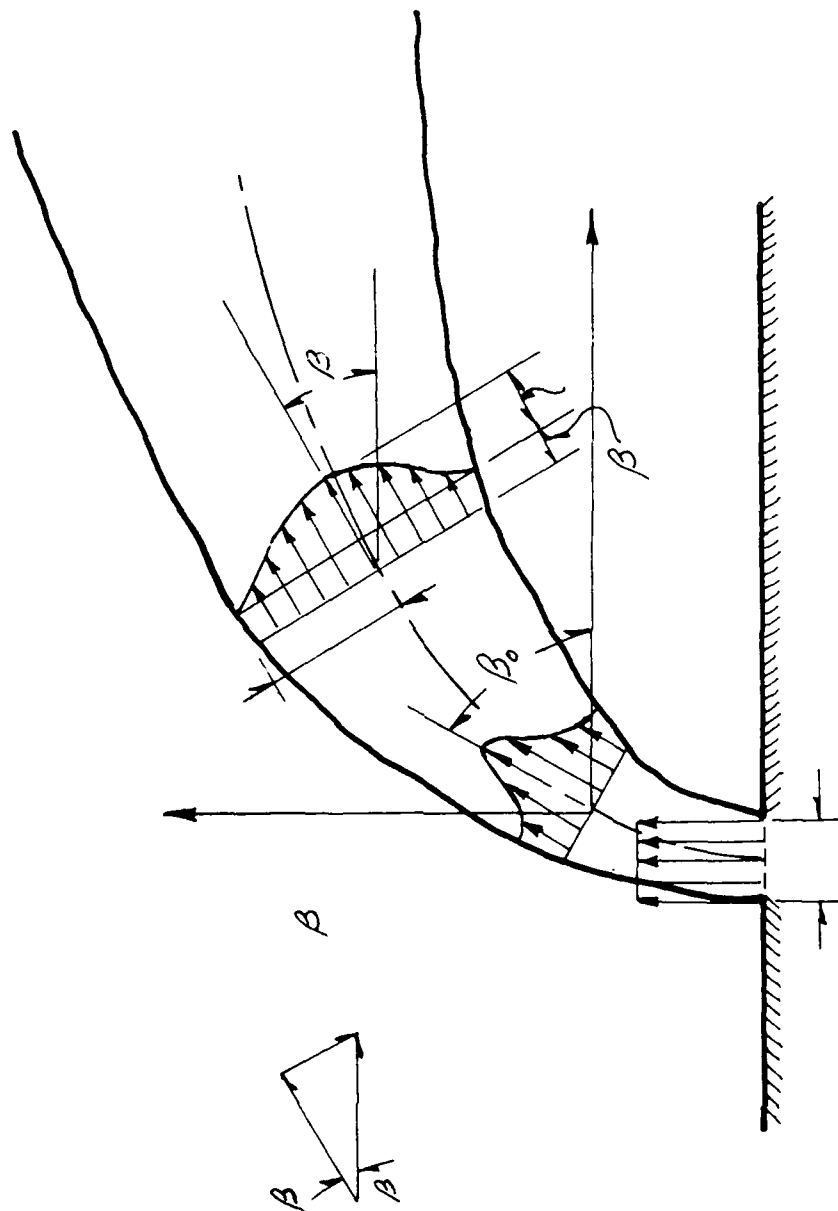


FIGURE 1 - SCHEMATIC OF JET PROBLEM

L = BOD excess at any point in jet cross section  
 $L_c$  = BOD excess (above ambient BOD) at jet axis

D = DO excess at any point in jet cross section  
 $D_c$  = DO excess at jet axis

Note that these profiles have the advantage over Gaussian profiles that they do approach a finite jet limit, such that ambient values are reached at  $\eta = b$ . The use of  $g = \sqrt{F}$  is based on Taylor's theory that scalar properties (heat, e.g.) are diffused more rapidly than is momentum.

In the use of integral analysis, an approach must be taken to consider the changing jet characteristics due to entrainment of ambient fluid by the jet. One approach is to specify the functional form describing the plume spreading rate. The method chosen here is the entrainment formulation. This formulation assumes that the rate of fluid entrainment into the jet is proportional to the jet centerline excess velocity,  $u_c$ . An entrainment velocity is postulated, representing an inflow velocity across the jet boundary, in the form

$$V_e = Eu_c \quad (8)$$

in which  $V_e$  = entrainment velocity

E = entrainment coefficient.

The assumption of similar profiles is usually considered valid only after some initial region, called the zone of flow establishment (ZOF), during which mixing proceeds from the jet boundaries to the axis and the profile is established. Therefore, the portion of the model assuming similar profiles can only be employed from the end of the ZOF. As shown in Figure 1, the jet may have experienced considerable bending and some dilution and widening. The model in the beginning will use available empirical evidence presented by Motz and Benedict (14) to define the length of the ZOF, and the angle and jet width at the end of this zone.

It has been recognized that the pressure differential existing across the jet plays a significant role in causing jet bending, and it will be presented here as a drag force (similar to Fan (15)) of the form

$$F_d = \frac{\rho_a C_d U_a^2 Z \sin \beta}{2} \quad (9)$$

in which  $\rho_a$  = mass density of fluid.

$C_d$  = drag coefficient

Z = vertical dimension of jet

The first version of the model assumes a uniform ambient current in the receiving water, as well as using constant values of the coefficients E and  $C_d$  along the axis. These could all be changed rather simply if later study shows it necessary.

#### EQUATION DEVELOPMENT

Space does not permit full development of all equations, but the process will be illustrated by use of the conservation of mass principle. Here, this simply states that the rate of change of the volume flux along the jet axis must equal the rate of entrainment of ambient fluid.

Entrainment is assumed to occur over the full depth of both sides of the jet, for a total length of  $2Z$ . This expression becomes

$$\frac{d}{ds} \left[ \int_{-b}^{+b} uzdn \right] = 2Z E u_c \quad (10)$$

in which  $s$  = distance along jet axis

Substitution of the velocity expression from Equation 3 enables integration of Equation 10 to yield

$$\frac{d}{ds} \left[ b \{ U_a \cos \beta + I_1 u_c \} \right] = E u_c \quad (11)$$

The jet depth,  $z$ , has been cancelled out of the equation. If  $z$  were a variable, the form of Equation 11 would be different and include some function of  $z$ . The constant  $I_1$  represents integration of the polynomial from Equation 3.

The momentum flux is resolved, for convenience, into its components along the  $x$  and  $y$  axes. Two factors which act to change the momentum flux are (1) the entrainment of ambient fluid which has its own momentum flux (in the  $x$ -direction) and (2) the drag force.

Integration of the two momentum equations yield the following

$x$  - momentum

$$\begin{aligned} \frac{d}{ds} \left[ b \cos \beta \left\{ U_a^2 \cos^2 \beta + 2I_1 u_c U_a \cos \beta + I_4 u_c^2 \right\} \right] \\ = E u_c U_a + \frac{C_d U_a^2 \sin^2 \beta}{4} \end{aligned} \quad (12)$$

y-momentum

$$\begin{aligned} \frac{d}{ds} \left[ b \sin \beta \left\{ U_a^2 \cos^2 \beta + 2I_1 u_c U_a \cos \beta + I_4 u_c^2 \right\} \right] \\ = \frac{-C_d U_a^2}{4} \sin \beta \cos \beta \end{aligned} \quad (13)$$

The geometric relations between length changes along the jet axis and y and change yield two geometry equations.

$$\frac{dx}{ds} = \cos \beta \quad (14)$$

$$\frac{dy}{ds} = \sin \beta \quad (15)$$

Equations 11, 12, 13, 14, and 15 describe the hydrodynamic behavior of the jet. Solutions of these equations as a unit yield the jet trajectory, velocity, width, and therefore the dilution it undergoes. An equation must be added to this set for any water quality parameter of interest. The flux of any parameter along the axis may change due to entrainment of ambient fluid containing quantities of that parameter. In addition, for non-conservative substances, there will be sources and sinks, such as those defined in Equations 1 and 2 for DO and BOD. Integration of these equations yields the following equations for BOD and DO respectively.

$$\begin{aligned} \frac{d}{ds} \left[ b \left\{ U_a L_a \cos \beta + I_1 L_a u_c + I_2 L U_a \cos \beta + I_3 u_c L \right\} \right] \\ = E u_c L_a - K_1 b \left\{ L_a + I_2 L \right\} \end{aligned} \quad (16)$$

in which L = centerline BOD excess above  $L_a$

$$\begin{aligned} \frac{d}{ds} \left[ b \left\{ U_a D_a \cos \beta + I_1 u_c D_a + I_2 D U_a \cos \beta \right. \right. \\ \left. \left. + I_3 u_c D \right\} \right] \\ = E u_c D_a + K_1 b \left\{ L_a + I_2 L \right\} - K_2 b \left\{ D_a + I_2 D \right\} \end{aligned} \quad (17)$$

in which D = centerline DO deficit excess above  $D_a$ .

In all equation,  $I_1 = 0.450$ ,  $I_2 = 0.600$ ,  $I_3 = 0.368$ , and  $I_4 = 0.316$ . All values result from integration of the various polynomials.



## SOLUTION OF MODEL EQUATIONS

The system of 7 equations has been non-dimensionalized and utilized in a computer program to provide solutions to the equations. The solution is obtained by a fourth order Runge-Kutta technique obtained from the IBM Scientific Subroutine Package. However, many other integration routines could be used. The system is well behaved and has no known singularities within typical discharge configurations and receiving streams. As a result, higher order numerical integration schemes are really not necessary.

To operate the model, a number of input parameters must be provided, as shown (see elsewhere for definitions).

Physical features of discharge:  $b_0, \beta_0, U_0, L_0, D_0$

Physical features of receiving stream:  $U_a, l_a, D_a, K_1, K_2$

Empirical jet coefficients:  $E, C_d$

Beginning work has been using values of  $C_d = 0.5$  and  $E = 0.05$  following recommendations of Benedict, et al and Stolzenbach and Harleman.

## PRELIMINARY RESULTS AND ONGOING WORK

The model has been applied to a few simple cases similar to those modeled by Rood and Holley (7). Initial computer runs reveal significant deviation from 1-D behavior in some instances. However, high degrees of early jet mixing tend to make the deviation less than that predicted by Rood and Holley (7). The important matter here is that significant portions of the stream may be subjected to substantially higher oxygen deficits than shown by the 1-D analysis. From the standpoint of model predictions, it appears that jet discharge angle may have only limited influence within certain ranges of angles. Practically, of course, the jet angle is of importance in determining possible jet impingement on the near or far bank. Some of these results will be presented again (they are available in Reference 1) as part of later discussions.

## RESEARCH OBJECTIVES

The purpose of the research which results are reported herein is to take the existing model and improve it and better understand its behavior. Several specific tasks exist in further development of the model. The empirical relationship used for the zone full establishment will be reviewed and improved to assure a better beginning point for the model. Elements which will be added to the model include a sedimentation term to allow for the deposition of solmentales which might be carrying a wasted strain being discharged. In addition, the model will be utilized for materials and properties other than BOD and DO, such as nonconservative substances and temperature. This will not only illustrate its extension to other constituents but also enable it to be verified against data that exists for these other properties, especially heat.

Since the model is an integral, one of the major problems is the influence of any surrounding boundary. A review of available literature will be made and recommendations presented for improvement of the model to handle these complexities. The areas of concern are the nearbank and the farbank. In some discharge conditions, both banks may influence the mixing. Primarily these boundaries decrease available dilution water and decrease mixing.

Sensitivity of the model to various input parameters will be reviewed with an eye to understanding the influence of these parameters on the model and the degree of accuracy required in their specification. This sensitivity analysis will necessarily be a preliminary one, for future improvements of the model may preclude some of the decisions made from a full scale analysis.

The model will be fitted to data obtained in situations where discharges have been made into two-dimensional flow conditions, but where the channel bottom restricts mixing and the jet begins by covering the full depth of the receiving water channel. These results will be chosen because the model as it exists is a two-dimensional model and therefore should be limited to those cases where this sort of behavior is expected to prevail. It is believed that a review of the model performance in comparison with this data will provide a number of useful understandings.

The conclusion of the work will be a statement concerning the applicability of the model, its reliability and sensitivity, and work which might continue in the future to develop the model to become even more useful.

## SECTION II BOUNDARY INFLUENCES

As noted earlier, the primary constraint in the use of any integral method is the fact that they fail to account for the boundary influences, with special interest here on the farbank and nearbank. The purpose of this section is to review the possible influences and some available understandings of the behavior of a discharge where boundary influences are important. This is expected to lead to possible suggestions for ways to modify the model as well as guidelines for its intelligent application.

### PROBLEM IDENTIFICATION

#### INTERFERENCE BY NEAR BANK

An obvious place where the shoreline has an influence exists when the plume is bent up against or very near the shore. In most river systems this happens eventually to all plumes, although in wider rivers it may be that the plume of discharged material is sufficiently far from the bank before it becomes parallel to the ambient current that the nearbank has no influence. In smaller streams it almost always will.

Figure 2 illustrates schematically the behavior occurring in the near shore region. The process can be viewed as one in which the shoreline limits water for mixing, as no water can be drawn across the solid boundary. In addition, however, it is really a competition for the water that is there. The review of Figure 2 illustrates the concept of reentrainment and recirculation. The jet in its early regions is striving to entrain surrounding fluid. On the inside, where water is limited, the only water which is really available is water which has already been entrained by the jet. This tends to set up a pattern of recirculation as shown in Figure 2. This means that water which has been entrained once and its level of the constituent of interest changed within continues to be entrained again. Therefore, the jet will entrain strictly ambient fluid from one side and material which has already been contaminated on the other. As one can imagine, these fluid flow phenomena are very difficult to describe mathematically.

One fact which is very important in the behavior of the plume in the region between the plume itself and the near bank is the depth of the plume relative to the surrounding fluid. If the receiving water is very deep and there is an extensive passage way beneath the jet, ambient water may be drawn into the jet as entrainment occurs by moving beneath the jet into the inner region. On the other hand, if the jet occupies substantially the full depth of the receiving water body, there is no means for available water to traverse to the region near the bank and then be entrained. In this latter case, the rate of reentrainment is considerably greater.

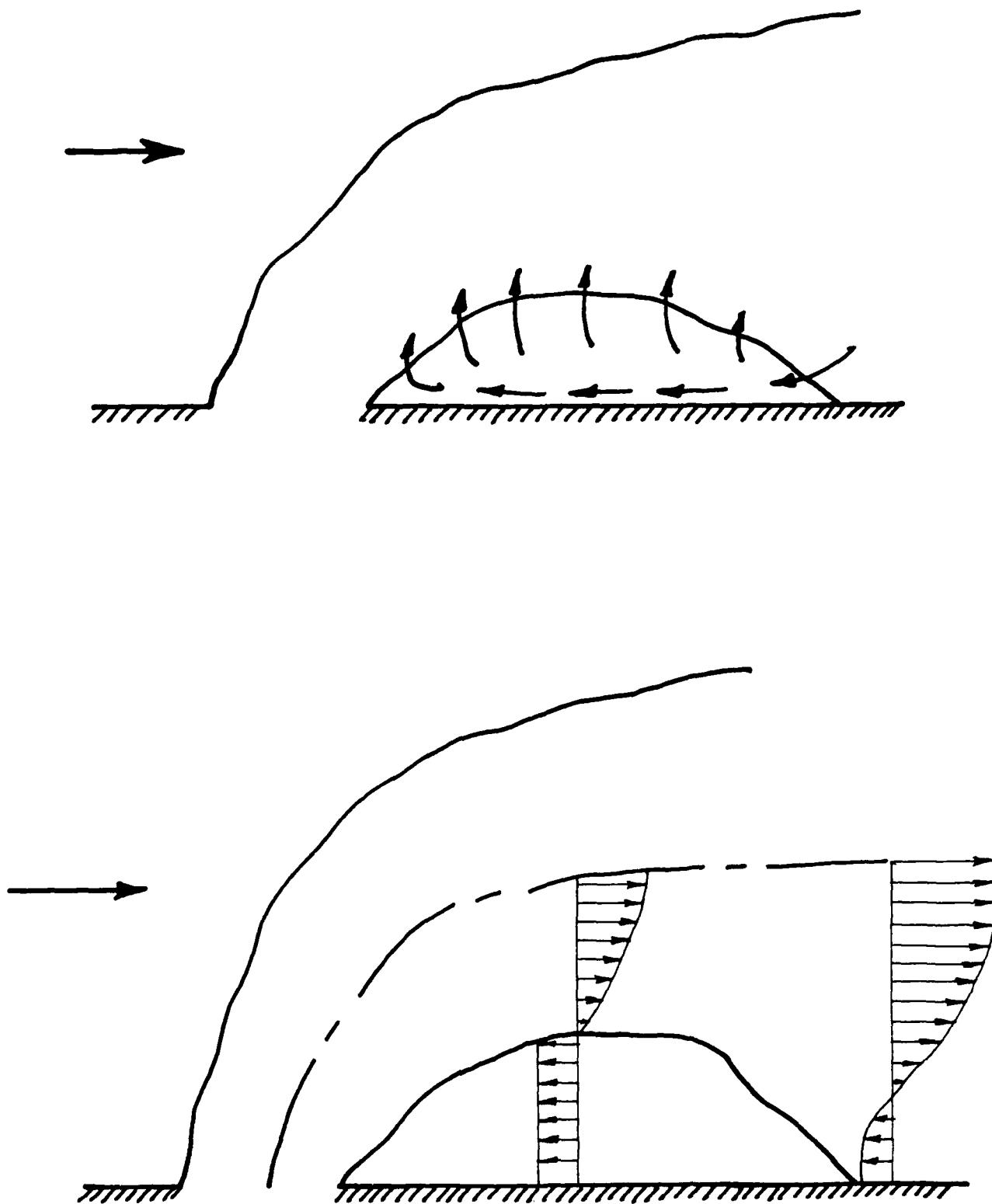


FIGURE 2 - NEAR SHORE BEHAVIOR

and the resulting concentrations of material are also greater near the bank. It should be noted that these depth effects are also very important in determining the trajectory of the plume. Plumes which cover essentially the full depth of the receiving water channel are more likely to be pushed against the shore than are those which occupy only a small portion of the depth. This phenomenon can be viewed as a drag force behavior similar to the distinction between a very blunt body placed in the wind and a more streamlined body.

In either the jet or the streamline body, the ability for fluid flow around the obstacle enables the fluid flow to decrease the pressure differential between the front and back of the body, thereby reducing the drag coefficient. Carter and others (16) have reported jets bending back toward the shore where they covered the full depths of the receiving water body. This behavior has been observed frequently in a class of flows known as reattaching flows. Sawyer (17, 18) and Abramovich (12) present examples of these flows. It seems clear that the limitation of available dilution water behind the plume not only diminishes the mixing and slows reduction of constituent values, but it also seems to attract the plume toward the boundary. Maxwell and Pazwash (19) have observed the same phenomenon near the water surface when a nonbuoyant discharge moved toward the surface, apparently due to limited dilution water. As noted by Adams (20), this movement toward the boundary is known as the Coanda effect. He presents numerous other examples from the literature of this type of behavior. One such example of special interest in waste discharges is the study performed by Liseth (21) with plumes entering from a multiport diffuser on opposite sides of the diffuser and merging at some distance above the diffuser pipe. Adams (20) has undertaken probably the most ambitious treatment of a discharge corresponding to the current study, treating a three-dimensional integral model. However, the model assumes a uniform concentration within each cross section of the plume, precluding the ability to present a detailed representation of the waste effluent distribution in the stream. Adams attempted to modify the standard integral approach to continually check for the closeness of the plume to the channel bottom. Entrainment was allowed to proceed at different rates on the two sides of the plume with the rate of entrainment and the temperature (Adams dealt with heated water discharges) of the entrained water being variable. Adams' work represents a useful point of departure, for it begins to look at the mechanisms involved in the problem. However, the model has not been well verified, especially where the ambient velocity is substantial. In addition, one must consider the practical drawback of not being able to predict the lateral variation of constituent concentration. Contact with Adams at MIT indicated that his model computer program was not in sufficient condition to be released, and therefore consideration that was given to obtaining that program and reviewing results with it had to be discontinued. From the standpoint of the intended output of a near-field water quality model such as the current model, no really useful information can be derived where these constituent distributions cannot be predicted laterally.

Another topic which has been treated in the literature in a variety of fields which has some bearing on the near bank problem is behavior of the so-called wall jet, or a discharge moving along the wall but having a different velocity from the ambient fluid.

Figure 3 illustrates typical behavior in a wall jet, without regard for how the jet became attached to the wall. This may have occurred in a variety of means. One can then compare Figure 2 with Figure 3. It can be seen that these two descriptions of the jet behavior are only the same at some distance downstream. Within the period of recirculation, there is a velocity at the wall which is flowing back toward the jet origin. In the established wall jet region, however, all velocities are directed downstream. As can be observed in Figure 3, the velocity at the wall and very near the wall is depressed because of the frictional resistance of the wall. This is an important consideration to make in terms of approximating the behavior of a plume as if it were a wall jet.

It should be observed that in cases where the ambient velocity and the jet discharge velocity are very similar, the rapid bending of the plume really puts the discharge quickly into a mode where it is basically a diffusion discharge and the jet model is really not needed. However, situations do exist where there is sufficient difference in the jet velocity and ambient velocity that a substantial region of mixing will occur at a rate other than due to ambient turbulence. This can be true especially in the case where the ambient velocity is significantly greater than the jet discharge velocity. This can be viewed as some sort of a reverse jet. This problem has not been well handled to date. Sayre and his coworkers at Iowa have presented several works (22, 23) which make use of diffusion model after some very short region of initial dilution. This initial dilution region is defined by empirical relationships based on data primarily. Benedict et al (8) presented a simplified analytical view of the behavior of such a discharge, but it really does not properly account for the existence of the wall. Among works which discuss various aspects of wall jets, including those resulting from the impingement of a jet on a solid boundary are those by Abramovich (12), Rajaratnam (24), Beltaos and Rajaratnam (25), Eskinazi and Kruka (26), Pande and Rajaratnam (27), Schwarz and Cosart (28), Stoy et al (29) and others. A couple of other interesting papers which deal with the effect of entraining walls include those by Hill (30) and Stoy and Ben-Haim (31). These later papers come from the mechanical engineering field.

Jirka et al (10) have reviewed available data and made a suggested criterion for attachment of the jet to the near shore. This criterion is defined by Equation 18.

$$\frac{U_a}{U_0} > 0.05 \left( \frac{h_{\max}}{H} \right)^{-3/2} \quad (18)$$

Equation 18 is really intended for discharges which are perpendicular to the shoreline and where the shoreline is straight. The maximum vertical extent of the jet is the depth which the plume would attain if the receiving water were infinitely deep. Therefore, it is possible  $h_{\max}$  could be larger than  $H$ . To the extent that the possible maximum depth equals or exceeds the receiving water depth, it can be seen that very little ambient current is apparently necessary to cause the plume to attach to the shore. If, as a simplification, one assumes that the maximum depth is equal to the surrounding water depth, it

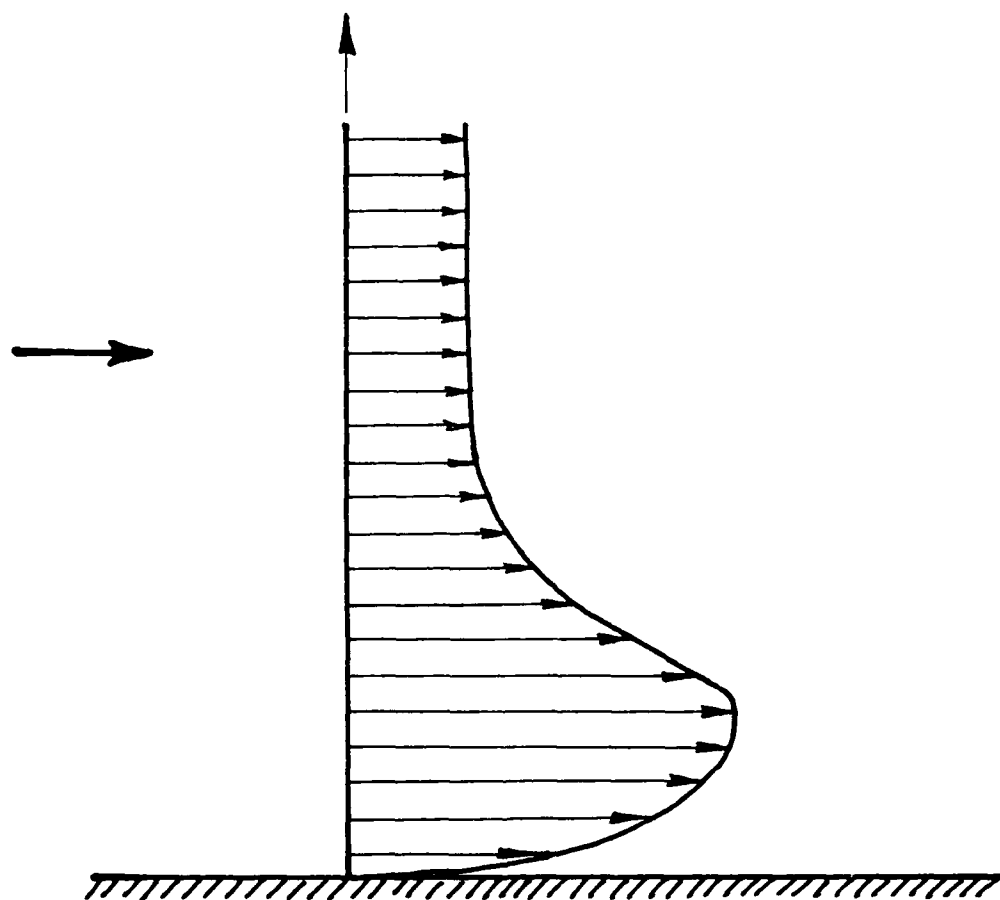


FIGURE 3 - WALL JET BEHAVIOR

can be seen that the plume will be attached to the shore if the ambient velocity is greater than or equal to five percent of the initial jet discharge velocity. All of this says simply that in cases where the jet initial depth is on the order of the receiving water depth, the probability is quite high that the plume would be attached to the shore. This sort of reasoning led Adams (20) to begin development of his work. One study on which he based some of his efforts includes a report by Sill and Schetz (32) and by Sacks et al (33). Both of these works deal with the influence of boundaries on surface discharges and provided a basis for some of the reasoning leading to Adams' model. Both Sill and Schetz (32) and Sacks et al (33) developed simplified models describing the gross behavior of the plume. The work by Adams actually represents an improvement of their efforts, but it still does not provide details of the concentration distribution within the jet region. It provides only a view of the longitudinal variation of some average value of parameters of interest.

The possibility of using existing wall jet evidence and equation formulations with the jet model is intriguing. Several steps will be necessary in order to incorporate this information into a jet integral model. Among those items which would have to be defined are the following.

1. Define the point of attachment of the plume to the shoreline.
2. Define the form of velocity profile both moving downstream and upstream from the point of attachment.
3. Define the changes in jet behavior as it nears the wall and begins to feel the influence of the wall but prior to the jet axis reaching the point of attachment as defined in Item 1.
4. Define the rate of entrainment in the region of reversed flow proceeding upstream.
5. Define the closure of the reverse flow region as it reaches the initial portion of the jet.

Items 1 and 2 can probably be reasonably defined from some of the references which have been presented, at least to the first approximation reasonable for this type of modeling. However, the ability to be very precise in handling any of the other 3 items mentioned is very limited at this time. The interaction in the region near the attachment point and near the point where the recirculating water approaches the beginning of the jet in the attached region is not very fully understood at this time. In addition, the ability to define the rate of entrainment in the full region, and especially its distribution along the length of the attached region, presents a problem. Sawyer (17) says that in one particular case approximately 60 percent of the entrainment occurred on the outer region of the jet and the 40 percent on the inner boundary. This ratio would clearly be a function of the pertinent jet discharge characteristics, including the velocity ratio, the Froude number, the aspect ratio, and the angle of the discharge.

The complexities of the physical behavior in this region are sufficient to cause concern. Of especial concern, at least to this author, is the question of whether one should modify an integral model by attaching a continuously varying profile. It seems to be getting away from the basic premise of the integral model. It has been noted by some authors that it is very possible to



go out on a limb by making unwarranted assumptions in an already simplified model. It might well be that the effort involved in properly incorporating these terms in an integral model would be comparable to that involved in attempting to handle the problem by numerical modeling of the proper differential equations for the system, thereby attempting to define the velocity field which would exist and the resultant entrainment. Realizing the goal of the current model as a planning and assessment tool, as opposed to a detailed research and analysis tool, it seems more reasonable to attempt to define other means of accounting for the walls' existence which are more consistent with these goals. It must further be recognized that where water quality constituents such as DO and BOD are decaying at some rate with time the relative accuracy in similar terms must be considered. It may be very difficult to put a very good value on the time rate of decay of a particular material, thereby minimizing some of the gain achieved by additional detail in the model. Therefore, it is recommended that this information on wall jets not be pursued in terms of the current model, although at a later stage, one might well consider it as a component in a three-dimension model where the localized effects are extremely important and where values of input parameters are more certain.

#### INTERFERENCE BY FAR BANK

Before discussing a number of the other techniques which are available for handling boundary influences, it is appropriate to mention the influences exerted by the far bank of the river. This is so because a number of the techniques might have application for either interference by the near shore or by the far bank, or perhaps both. In fact, the wall jet which has already been discussed might be utilized for treatment of jet once it has struck the far bank.

In a typical situation, confinement by the far bank of the river has some distinct differences from the situation which exists where the near bank is the factor. The very distinct zone of recirculation which can exist on the near bank is unlikely to exist in common river systems on the far bank. This is because the plume has bent downstream and simply has no trapping of material and subsequent reentrainment and recirculation behind the plume. Of course, if unusual geometry existed, such as shallow embayments attached to the side of the main river, then such zones might exist on the far bank. However, it is believed more likely that the far bank problem would reduce itself to being a jet impingement problem. In this sense, to approximate the behavior of the plume as a wall jet once the far bank has been reached would be more justifiable on the far bank. At and near to the point of impingement, dilution of the discharge is restricted because of the lack of dilution water. In addition, the far bank exerts a frictional influence retarding flow in the jets and exerts a solid body external force just as any structure being hit by jet fluid. The resulting force exerted by the wall forces the jet to move directly downstream. The problem seems much simpler in those cases where the plume has been bent downstream sufficiently to minimize the angle as well as the excess velocity existing at impingement. If the jet approaches the far bank in a very small stream at near 90°, the problem would be extremely complicated because of reverse flows upstream of the impingement point. Of

course, it is also true that if the jet velocity is nearing the ambient and is approaching the far bank at a shallow angle, then diffusion models might be appropriate instead of jet models in any event. The next portion of this section will discuss a number of techniques which might be utilized to handle geometry influences for either near or far banks.

## OTHER METHODS FOR APPROXIMATION OF BOUNDARY INFLUENCES

### USE OF IMAGE SOURCES

The method of images has been utilized in a variety of fields to obtain solutions to the convective-diffusion equation, as well as the Laplace equation. This technique has been used in ground water hydraulics, diffusion problems, heat transfer, electrostatics, and optics among others. The principle says that solid boundaries can be approximated by placing one or more imaginary, or image, sources which yield surfaces across which there is no flow. These surfaces then represent the solid boundaries, which are also no-flux boundaries. The ability to add solutions to obtain another solution is dependent upon the equations being linear. The diffusion equation and the Laplace's equation are linear. Reference to Equations 12 and 13 in Section I reveals that the momentum equations for the jet problem are nonlinear. This means that in the strictest sense one should not be able to add two solutions together and obtain a solution to the equations. Two workers have made use of the method of images, and a review of their work is instructive. Maxwell and Pazwash (19) and Wu (34) both employed this method.

Maxwell and Pazwash (19) dealt with a nonbuoyant discharge into a stagnant ambient medium. The discharge is directed initially parallel to the boundary of interest, usually the water surface. Therefore, when utilizing the image approach, the authors were dealing with a discharge which was parallel to the boundary of interest and therefore had no velocity component to be added in the jet solutions which were at some angle to the boundary. They found a very interesting result. When they added the solutions together for the nonbuoyant discharge, they found a velocity field which moved toward the surface. The plume actually behaved as one might expect a buoyant discharge to behave, that is rising toward the surface because of the lighter fluid. This effect is undoubtedly similar to the Coanda effect discussed earlier in conjunction with the decrease of pressure behind the plume and resultant reattachment of the plume to the shore. Evidently if the discharge is sufficiently close to the surface or the bottom the limitation of available dilution water results in a movement of the plume toward that boundary.

Wu (34) utilized an image approach which forced his plume to be totally contained within the receiving water boundaries both vertically and horizontally. Wu developed a model which combined an initial jet region and a diffusion region. He made some simplifying assumptions to approximate the solid boundary by the method of images. He observed that there will be large discrepancies in the wall region very near the solid boundary as compared to the actual concentration and velocity distributions which would exist in that region. Wu defines the end of his jet region as the point at which the jet centerline excess velocity is less than 10 percent of the ambient velocity and also the angle of the jet with respect to the ambient current is less than  $25^{\circ}$ . This model developed a

circular discharge, although modifications probably could be made. Once the diffusion solution is begun the method of images approach can be applied with more certainty.

It is clear that the method of images solutions would not handle situations where there is an angle of approach of the jet toward the boundary. In addition, it clearly does not account at all for the recirculation and reentrainment noted as being important on the near bank. The inability to properly account for the velocity immediately at the wall is difficult to assess as to the impact on the final results. It appears that this technique has some value for application to the jet regions on the near and far beyond the point where the recirculation pattern is established. At this time, however, it is unclear that the complications involved with addition of the images to the model would sufficiently improve its capabilities in the view of the further shortcomings to make it a worthwhile expenditure of time and effort.

#### SCHEMATIZATION OF DISCHARGE

An approach which has been suggested for some discharges attempts to simplify the geometry conditions near the discharge. Stolzenbach and Harleman (13) show a number of possible situations which might occur. Basically it is intended to treat a discharge which is either directed immediately down the shore or is bent so rapidly against the shore as to be essentially of that form. The treatment assumes the discharge is directly down the shoreline with a width equal to twice the physical discharge width, with the jet centerline located on the shoreline. This then yields a jet prediction which shows spreading both ways. Then that portion of the jet outside the physical boundary is simply disregarded and the half jet in the water body is considered to be an approximation of the actual discharge behavior. This sort of circumstance might occur in rapidly flowing streams (although in these cases the discharge is not truly a jet) or in cases where the discharge angle is very shallow, approaching zero. Additionally, if an island or other structure exists immediately out from the discharge point, it may well be that the initial discharge will strike this obstruction and immediately move directly downstream, thereby simulating a discharge essentially oriented directly down the shoreline. A review of the earlier figures will indicate that schematization has difficulties common to some of the other methods which have been discussed. This schematization does not really account for the velocity field that develops between the jet and the near wall. Even if the jet were actually directed down the wall and no obvious zone of recirculation were established in a trapping region between the jet and the wall, the velocity profile typical of a wall jet would not be observed. Schematizing the discharge in this section would yield the peak velocity at the wall. In the real system, friction against the wall would reduce the velocity in that near region. The very fact that wall friction is neglected may also have a significant impact upon the deceleration and dilution of the plume.

Another question arises when the discharge is schematized. If real mixing occurs only on one side of the jet in the physical system, is it proper to reduce the entrainment coefficient, perhaps even dropping it to one-half the usual. There is indication that such a step is called for to yield adequate

results. It is uncertain whether it should be a 2 to 1 ratio or whether there should be some other change made in the coefficient. This question is clouded by the comments made about the inadequate description of the velocity field in the plume.

It is believed that schematizing the discharge can provide useful results in some instances. In fact in very complex situations it may be the only way to obtain any sort of reasonable results at all. This schematization of the discharge really does not involve any further development of the model, but rather simply application of it with proper input parameters. The one item that would need investigating is the possibility of changing the entrainment coefficient to make better sense of the results. Because of the possible utility of this method, it would be investigated in a further section of this report. It should be recalled, however, that there are reasons why this approach has its limitations and should be employed with caution.

#### LINKAGE OF JET AND DIFFUSION MODELS

A few references have already been made to the point at which the discharge plume no longer behaves like a jet and can be considered to be dominated by ambient diffusion processes. At this point, the description of the discharge is presumably best handled by a solution to the convective diffusion equation. There is still a good deal of uncertainty as to the point at which this diffusion phenomenon becomes dominant and should be used in modeling the discharge. Abramovich (12) had indicated that where the maximum plume velocity differs from the ambient velocity by no more than 8 percent it is almost impossible to distinguish between the two. Various authors have used different points, usually arbitrarily chosen to some extent on velocity considerations. Jirka et al (10) have suggested that the end of the jet be considered the point at which the excess velocity (above ambient) in the jet had been reduced to 10 percent of the initial excess. It seems important that the absolute magnitude of this difference be considered as well. Typically, it is very difficult to distinguish between velocities which differ by 0.2 feet per second or less in a river. This is especially true if the discharge plume covers a sufficient width of the river to be exposed to quite different velocities. Therefore, in cases where the discharge velocity is rather close to the ambient velocity, a reasonable cutoff point may occur where a good deal more than 10 percent of the initial excess velocity remains. On the other hand, where the jet is very strong with a very large initial excess velocity, it may require going further downstream to the point where the percentage of the initial excess is less than 10 percent. In any event, there are no firm guidelines in this matter. One portion of the work of this report will attempt to review some of the behavior and to define some guidelines.

One model commonly used for thermal discharges is the PDS model by Davis and Shirazi (35). This is a three-dimensional model which includes the diffusion as a form of additional entrainment and turbulence. Some workers, for example Jirka et al (10), have criticized this approach, suggesting that the additional terms should not be included in the momentum and mass balance equations but instead in the equations for the constituents of interest, such as BOD. The inclusion of this additional entrainment in the model allows the jet model to continue calculations well past the point where the plume has discontinued

being a jet, by whatever definition one uses. This may be useful in some circumstances; however, if the discharge plume reaches the banks and these boundaries begin to play a significant role, then the inability of the model to account for such boundaries again makes it inadequate. Therefore, at this point a model which accounts for the finite boundaries and represents the solution to the convective diffusion equation should be used. The direct inclusion of ambient diffusion in the model also enables one to account for varying degrees of ambient diffusion which might interact with the initial jet discharge, especially where highly turbulent streams exist.

Lau (36) has utilized a simplified patching together of jet and diffusion solutions. He utilized the Stolzenbach and Harleman (13) jet model and took the width, depth, and excess temperature existing in the plume at the end of the defined jet region. This enables him to define a new source of finite size at the end of this region which serves as a source for a solution to the ambient diffusion problem. This particular technique is useful but it has the disadvantage that the profile at the end of the jet region is redistributed over a plane source of uniform concentration. Therefore, there is a discontinuity at the point where the diffusion model begins. This particular problem is common to many of the techniques which have been suggested, although a more realistic approach would be to utilize a distribution for the diffusion model which is predicted by the jet at the end of the jet region. Other workers have attempted to patch together solutions in a similar context. For example, Sundaram (37) put together a simplified view of plume trajectory and temperature decrease for a thermal plume based on equations from smokestacks and patched this into a diffusion model. However, Benedict et al (9) noticed that the model gave inconsistent results for some cases. It was especially noted that the equations which help provide the description of the jet did not perform adequately.

A series of stream-tube models adds strength to models that have been developed for rivers. The basic premise for these models is given in Yotsukura and Cobb (38) and Yotsukura and Sayre (39). Basically, the equation for conservation of mass of fluid is used to replace the lateral coordinate from the bank by the cumulative discharge measured from the bank. The cumulative discharge is the total discharge between the bank and the point of interest in the river. Therefore, the cumulative discharge has a zero value on the nearbank and increases to the full river discharge at the far bank. Several reports of data in these references indicate that data which is plotted as concentration versus cumulative discharge gives a very close approximation to a Gaussian curve even where channel geometry is not uniform. When manipulation is performed, and some simplifications are applied, the diffusion equation can be reduced to a 1-dimensional equation and solved by standard means. The concentration is then given as a function of the downstream coordinate and the cumulative discharge. If the velocity distribution in the stream is known or can be estimated, then a direct correlation between the lateral coordinate and the cumulative discharge can be found; then the concentration distribution can be put in terms of physical distances from the shore. Sium (40) has suggested a simple relationship as shown in Equation 19.

$$\frac{q}{\bar{q}} = b_0 \left[ \frac{h}{\bar{h}} \right]^{b_1} \quad (19)$$

in which  $q$  = discharge per unit width at point of interest  
 $h$  = local depth at point of interest  
 $\bar{q}$  = average discharge per unit width at the section =  $Q/B$   
 $\bar{h}$  = average depth at the section  
 $Q$  = total river flow  
 $B$  = river width  
 $b_0$  = coefficient, usually between 0.8 and 1.0  
 $b_1$  = coefficient, approaches 5/3 as width-to-depth ratio of river increases

Equation 19 is largely based on data collected in the Missouri River. Additional work is required to more adequately define the parameters, but Equation 19 does provide a beginning point to approximate the velocity distribution in any section of a river based purely on the depth variation across the river. This is very helpful, for it is much easier to measure the depth than the velocities in the river.

Sayre and his colleagues at Iowa have utilized the stream tube model for studying thermal discharges in the Missouri River and other similar, relatively shallow streams. Essentially, they dismiss the jet region entirely, for they are dealing with systems in which river velocity is greater than the jet discharge velocity and the plume has immediately bent against the shore. They treat the jet region by merely specifying an initial dilution due to the jet and using this as a beginning point. Here again, the source consists of a uniformly distributed temperature in the beginning which may not be entirely realistic in all cases. However, this model should also be useful for linkage to an existing jet model. The stream tube model has the distinct advantage that it does incorporate the varying longitudinal velocity as one moves across the river. It has been assumed that these velocities are extremely important in the overall mixing process. A simple two-dimensional model has been developed by the USGS (41), linking the Motz-Benedict (14) model for the jet region with the stream tube model.

Another possibility for linkage to the jet region is the use of a finite source, similar to that provided by Lau. However, both Lau (36) and Sayre and Paily (23) deal with a shore-attached plume. In some instances, it may be that the plume has moved away from the shoreline before it is at the end of the jet region and it actually represents a diffusion source which is located at some distance from the river bank. In these cases it would be proper to have a description for sources away from the bank. Of course, the USGS model (41) discussed does exactly this, and the Iowa model could be modified to allow for off shore cases. Another possibility is to use a finite source direction presented by Prakash (42) and modified by Benedict (43). Equation 20 is the solution for a source discharging continuously into a uniform river flow.

$$c(x,y,z) = \frac{M}{4} \sum_{m=-\infty}^{+\infty} \sum_{n=-\infty}^{+\infty} e^{-\lambda x/u} \quad (20)$$

$$\left[ \begin{array}{l} \text{erf } A_1 - \text{erf } A_2 + \text{erf } A_3 - \text{erf } A_4 \\ \text{erf } A_5 - \text{erf } A_6 + \text{erf } A_7 - \text{erf } A_8 \end{array} \right]$$

in which M = rate of discharge of material;  $\lambda$  = decay coefficient  
 ( $K_1$  for BOD)  $A_1 = (y + y_2 - 2mB) / P$ ;  $A_2 = (y + y_1 - 2)$

$$\begin{aligned} A_3 &= (y - y_1 - 2nB)/P; & A_4 &= (y - y_2 - 2nB)/P; \\ A_5 &= (Z + Z_2 - 2mD)/G; & A_6 &= (Z + Z_1 - 2mD)/G; \\ A_7 &= (Z - Z_1 - 2mD)/G; & A_8 &= (Z - Z_2 - 2mD)/G; \\ B &= \text{channel width}; D = \text{channel depth}; P = 2 (D_y x/u)^{1/2} \\ G &= 2 (D_z x/u)^{1/2} \end{aligned}$$

One other thing that can be done is include transverse ambient diffusion in the basic equation directly. It was noted that the Prych-Davis-Shirazi (35) model incorporates ambient diffusion in the form of an additional entrainment. It is believed more proper to include the ambient diffusion term in the conservation equations for the constituents of interest, in this case Equations 16 and 17. Jirka et al (10) note that entrainment is usually considered as the incorporation of less turbulent ambient fluid into a highly turbulent zone, while ambient diffusion is the exchange of fluid masses with different concentrations but similar turbulent intensities. It is therefore recommended that in order to gain a view of the relative impact of these parameters, the term be included in Equations 16 and 17, and example runs completed in order to review the effects. One item of some importance in this consideration is the entrainment coefficient which has been determined for the jet model would include the effects of ambient turbulence.

#### SUMMARY OF APPROACHES AND LIMITATIONS

Several possible approaches dealing with the problem of boundary influences on the integral model have been reviewed. At all times it should be recalled that the existing model is a two-dimensional model and full scale development of some detailed behavior may be better directed until a time when the model is three-dimensional. In addition, improvements in the model should be made in light of its expected use and the further realization that minor discrepancies in the near field zone may not be critical in light of the time

required for the various biological and chemical reactions to occur. Approaches to dealing with the boundary problem fall into the consideration of the wall jet approximation, the method of images, schematization of the discharge, and linkage of the jet model with appropriate diffusion models. In these attempts one must deal both with the near shore and far shore phenomena. In near shore it is a particular problem of recirculation and reentrainment of the fluid as it is potentially trapped between the plume and the shore. A fifth methodology then is to attempt modification of the work done by Adams (20) which incorporates bottom and near shore influences and tries to include recirculation. However, Adams' work does not allow prediction of lines of equal concentration of the constituent of interest. It yields only a longitudinal variation of material.

Each of the techniques have something to offer. The discussions have attempted to focus on the relationship of the approximations to the actual physical behavior in the system. The most complex region by far is the recirculation and reentrainment regions on the near shore. Both the wall jet and method of images approaches have some theoretical basis, although neither one will clearly handle the recirculation region. Schematization in the discharge is really not an improvement of the model but rather an attempt to modify the input for particular conditions where the discharge may be directed down the shoreline. Further development of the model as limited in the two-dimensional form by including the wall jet and images approaches does not seem warranted at this time, especially in as much as these would probably not help very much in the definition of the complex recirculation problem. Schematization can be used with the model in whatever form it exists. Therefore, it appears at this time that the most promising approach from the practical standpoint is the linkage of the jet model with appropriate diffusion solutions which carry results downstream. Work to be reported in later sections of this report will show some comparisons between jet results and from several diffusion solutions. It will be seen that with proper care in selection of input coefficients, this linkage can provide very useful results for planning and assessment purposes.



### SECTION III ZONE OF FLOW ESTABLISHMENT

#### BASIC BEHAVIOR

The Zone of Flow Establishment (ZOFE) is a very important region in jet discharge problems. Figure 1 shows the zone which is that region in which the discharge with initially approximately uniform profiles of temperature, concentration, and velocity mixes with the ambient fluid and obtains profiles of the important properties which begin to look like Gaussian profiles. The classic discussion of behavior in the Zone of Flow Establishment occurs in the paper by Albertson et al (44). They note that in the Zone of Flow Establishment the moving jet is beginning to drag along the surrounding ambient fluid through the shearing action. This causes an acceleration of the surrounding fluid and deceleration of the fluid in the jet. As one proceeds further from the jet discharge, larger portions of the jet are decelerated. Eventually, the centerline of the jet is reached and subsequent to this point, the jet centerline velocity also begins to decrease. Therefore, up to the end of the ZOFE the jet centerline velocity remains unchanged. Other constituents may be assumed to behave in a like fashion, although later discussions indicate that the end of the ZOFE may not be the same for mass as it is for momentum.

The work by Albertson et al (44) indicated that for discharges into stagnant ambient bodies, the length of this ZOFE is about six times the diameter for circular discharges and about five times the slot width the rectangular slot discharges. Benedict et al (9) review available data and note the strong dependence of this length on the ratio of the ambient current to the jet discharge velocity. As the ambient current becomes a larger and larger percentage of the initial jet discharge velocity, the length of the Establishment Zone decreases. For a typical rectangular discharge, it appears that the length of the zone may be on the order of only one to three times the jet width, at least for situations where the jet velocity is less than two times the ambient.

A review of Figure 1 as well as the required input for a jet model indicates that the key parameters to be determined at the end of the ZOFE are the width of the plume, the angle of the plume with respect to the ambient current, and the length of the ZOFE (or the location of the end of this zone). These items are important for the jet integral equations do not apply in the ZOFE. This is because a review indicates that the polynomial expression used for lateral variation of constituent concentration and the velocity do not apply within the ZOFE. Therefore the three items indicated at the end of the ZOFE must be provided as input to the model. It is therefore important to make as good an estimate as possible of the conditions existing at the end of this zone. In this zone it is especially true that the bending can be very extreme, substantially changing the angle for input to the model.

## ZOFE TREATMENT IN CURRENT MODEL

As noted, in order to obtain a solution it is necessary to provide values of the parameters  $b_0$  and  $\beta_0$  at the end of the zone of flow establishment, in addition to values  $u_0$ ,  $L_0$ , and  $D_0$ , the excess value at the end of the ZOFE.

For the reduced angle,  $\beta_0$ , the data presented by Motz and Benedict (14) will be utilized. It is expected that these values will provide angles sufficiently close to actual to give useful results. Ultimately, sensitivity of the model to input angle will have to be reviewed, but these existing data will be used for current modeling efforts.

The initial velocity excess,  $u_0$ , at the end of the ZOFE is defined by

$$u_0 = U_0 - U_a \cos \beta_0 \quad (20)$$

in which  $u_0$  = initial excess centerline velocity at the end of ZOFE

$U_0$  = discharge velocity =  $Q_p/A_D$

$Q_p$  = total plant discharge

$A_D$  = area of discharge orifice

This merely recognizes that the total jet centerline velocity at the end of the ZOFE is still that which existed at jet discharge, or  $U_0$ . Values for  $L_0$  and  $D_0$  are simply found by subtracting ambient values  $L_a$  and  $D_a$  from discharge values  $L_0$  and  $D_0$ .

The remaining parameter needed at the end of the ZOFE is  $b_0$ , the jet half-width. The initial discharge half width is  $b_0'$ . It has been stated that different lateral profiles were chosen for the scalar properties than for velocity due to the faster lateral diffusion of the former. This has the effect of causing the ZOFE based on  $L$ , e.g., to end before the ZOFE based on velocity. This would mean that when this latter point was reached, the BOD would already be below  $L_0$ . However, little is known about this behavior in discharges into moving streams. Therefore, for the time being it will be assumed that the ZOFE has the same length by either definition. Fan (15) notes that this has the effect of underestimating the dilution of the scalar property, in this case BOD, probably by about 10 percent. Further refinement in this approach may be sought in the future, but the accuracy here is believed consistent with goals of the current work.

Using this assumption, and neglecting any decay of BOD in the ZOFE, the flux of BOD in the jet from the orifice can be equated to the flux of BOD in the jet at the end of the ZOFE. If ambient BOD,  $L_a$ , is assumed zero, this conservation equation becomes

$$2U_0b_0' - zL_0' = 2b_0zL_0 \{0.60 U_a \cos \beta_0 + 0.368 U_0\} \quad (21)$$

Using the definition given in Equation 21, it is possible to obtain

$$\frac{b_0}{b_0'} = \frac{1}{0.368 + 0.232 A \cos \beta_0} \quad (22)$$

in which  $A = U_a/U_0$

Equation 22 defines the relationship between the width at the discharge point and at the end of the ZOFE.

#### IMPROVEMENTS IN CURRENT DESCRIPTION

The two main features which have been identified as missing from the current model description of the ZOFE are the inclusion of a nonzero ambient BOD and inclusion of different rates of spreading and hence different lengths of the ZOFE for velocity as compared to concentration.

As noted earlier, there is uncertainty as to the relative rates of spreading of mass and momentum for discharges into a flowing stream. Stefan (45, 46) had investigated ZOFE behavior in heated water discharges. He notes (45) that in a free jet the transverse spread of excess water temperature is faster than that of velocity (momentum). The standard deviation of the transverse temperature profile is generally considered to be from five to ten percent higher than for velocity. As a result, the establishment length would be different by similar amounts. He states that it is believed that this is well within the error of measurement of the establishment length data. Therefore, he combined data derived from temperature and velocity measurements and analyzed them together. In short, his data made it difficult to distinguish between the two measures of the end of the ZOFE. Based upon this and similar findings reported elsewhere, it is believed appropriate at this time to disregard the possibility of the ZOFE ending at different points for the different properties. Therefore, the BOD concentration at the end of the ZOFE will also be considered to have a centerline value equal to the initial BOD at the discharge. The same assumption would be true for concentration of any other constituent of interest.

The inclusion of a nonzero ambient BOD,  $L_a$ , seems worthwhile. This would be especially true as increased levels of treatment diminished the difference between the ambient and the discharge concentrations. The procedure in developing a relationship will be as before, with the flux of BOD at the discharge point being equated to the flux at the end of the ZOFE. When this step is taken in a manner similar to that leading to Equation 21, the following equation results.

$$\frac{b_0}{b_0'} = \frac{1}{\frac{L_a}{L_0} \{0.082 + 0.312 A \cos \beta_0\} + 0.368 + 0.232 A \cos \beta_0} \quad (23)$$

Equation 23 can be seen to collapse to the form of Equation 22 if the ambient BOD is zero. Equation 23 then represents the more general relationship. This equation is valid for all cases in which the discharge BOD,  $L_0$ , is greater than or equal to  $L_a$ . If this condition is not met, the ambient BOD is greater than the discharge BOD. The polynomial profile would then be an inverse one. While it is possible that this might be useful for description of the problem, it is uncertain whether it is a good representation of the mixing phenomenon or not. In effect, this situation would be one in which the ambient river polluted the discharge. For practical values of  $L_0$ , the differences between Equations 22 and 23 are small. However, as treatment processes are improved to meet regulatory guidelines, the discharge BOD will approach the ambient, making Equation 23 preferable.

#### RECOMMENDATIONS FOR ZOFE

It is recommended that Equation 23 be utilized to describe the plume width at the end of the ZOFE. The angle and the length to the zone end will still be taken from the work by Motz and Benedict (14). It is believed that this level of description of the ZOFE is consistent with the utility of a two-dimensional model. If future work is undertaken to develop this model into three-dimensions, it is recommended that the proper conservation equations be written for the ZOFE and their solutions obtained numerically as a part of the overall solution. This approach is similar to that adopted by Stolzenbach and Harleman (13).

## SECTION IV INCLUSION OF OTHER PARAMETERS

### GENERAL MODELING

The equations developed for BOD and DO, as well as the methodology for their derivation, is similar to that which will be employed for any conservative or nonconservative substance. The BOD Equation (Equation 16) could be immediately adapted for any conservative substance by dropping the decay ( $K_1$ ) term and interpreting  $L_a$  as the ambient value of the substance and  $L$  as the centerline value. Essentially, in the current mode, the model could be operated for conservative substance by simply reading in the value of  $K_1$  as zero and then using the calculated results for BOD as appropriate for that constituent. Using the substance of interest as not conservative, it is directly analogous to BOD if the substance can be considered to exhibit a first order decay as shown for BOD. If this is the case, Equation 16 can be used directly for that substance with the proper value of  $K_1$  for the substance of interest included. If it developed that BOD and several other constituents were of interest, then the number of equations being solved by the model could be increased to include these additional elements. For example, if 5 additional substances were of concern, with 5 different decay coefficients, then 5 additional equations would be included. Each of the equations would have the form of Equation 16 with proper designations for the ambient and centerline values of the substance, with proper values for the decay coefficient included. The program could then be modified to include as many of these equations as necessary.

One substance or property of interest is temperature. As a first approximation, the decay of temperature to the environment can be assumed to exhibit a first order decay. The so-called equilibrium temperature concept is based on this belief. One of the reasons for looking at temperature is the data which has developed in the literature because of the interest in thermal pollution. In this respect, temperature losses to the atmosphere in the near-field, or jet, region are usually considered negligible. Therefore, an exact description of the decay process is probably not necessary in order to utilize the data for model verification. In fact, it may well be appropriate to simply assume that the temperature is a conservative substance for the verification process.

### INCLUSION OF BOD SETTLING

One additional mechanism for removal of BOD from the discharge plume is sedimentation, or settling out of solid particles which exhibit a BOD. This material then ends up on the stream bottom, where it may exert a benthic demand on the ambient waters. In addition, the material may be resuspended during times of higher flows in the river and therefore result in larger local and far field values for BOD and the resulting DO deficit. There are numerous

approaches to inclusion of this settling out. The first of these would be the introduction of a single, constant coefficient  $K_3$ , similar to the coefficient  $K_1$ . This coefficient would be included in the term essentially the same as the  $K_1$  term in the Equation 16 for BOD. This approach assumes that the deposition rate is independent of the fall velocity of the particle or the velocity of the jet, at least directly. Another approach would attempt to make the coefficient  $K_3$  a function of the concentration of BOD and the fall velocity of the remaining particles. This approach would attempt to account for the fact that the larger particles settle out first, leading behind particles of different fall velocity. A third possible approach would make the coefficient  $K_3$  a function of the centerline velocity of the plume, recognizing that a given particle would settle more rapidly in slower moving water.

Each of the approaches has something to offer. The use of a single, constant value of  $K_3$  may not be the most realistic for several reasons. However, use of such a value does at least yield a system in which deposition of material decreases as one moves along the plume to the point where smaller particles remain in suspension and as the jet velocity decreases. In addition, it may very well be that this simpler approximation of the behavior is consistent with the two-dimensional character of the existing model. Therefore, it is recommended that sedimentation be included as an additional term in Equation 1 of the form as  $K_3L$ . This would then result in an additional term on the right hand side of Equation 16, given as the following.

$$\begin{array}{l} \text{Added term for} \\ \text{sedimentation} = K_3b (L_a + 0.600 L) \end{array} \quad (24)$$

The additional term indicated by Equation 24 provides increased ability to describe BOD behavior if one knows the constituents and the rate of sedimentation. It is realized that this is a simplified view of the process, but further work might justify inclusion of more detailed descriptions. For the time being, however, this should provide a useful description of another pertinent process in the near field description of water quality behavior.

## SECTION V

### DEFINITION OF END OF JET REGION

#### LIMITATIONS TO JET MODEL

The Model as it currently exists describes a two-dimensional plume, with no vertical mixing. This may occur due to the existence of a solid bottom which limits mixing or due to buoyancy forces which restrict vertical mixing due to a density gradient. One limitation to the existing model then occurs if the system is three-dimensional and buoyancy controls or when buoyancy forces are no longer sufficient to prevent vertical mixing. This then represents an effective end to applicability of the jet model.

A second consideration in defining the end of the jet region is more universally applicable. As the centerline excess velocity in the plume approaches zero (that is, the jet velocity approaches the ambient) the model will show small or zero mixing. This is because the only mixing mechanism included in the jet is entrainment. The mixing is determined by multiplying the entrainment coefficient by the centerline excess velocity. As this centerline excess velocity becomes small with respect to the ambient velocity, it seems clear that ambient turbulence might begin to be the dominant feature in the mixing of the plume. Therefore, one can visualize a point at which the jet model becomes inadequate because it does not account sufficiently for ambient turbulent diffusion. It is the definition of this point on which most emphasis will be placed in defining the end of the jet region in this report.

#### PREVIOUS DEFINITIONS OF JET ENDING

A number of investigators considered the question of the end of the jet region. Several of these have been mentioned previously and will only be repeated here briefly. Benedict et al (8) suggest that when the jet velocity is on the order of 1.20 times the ambient then the discharge may be properly considered as a diffusion discharge in most cases. Jirka et al (10) suggest a criterion that the initial centerline excess velocity be reduced to 1/10 of the initial excess. It has already been mentioned that this later definition must be coupled with some measure of the absolute value of the velocity excess involved, remembering that velocity differences on the order of 0.1 to 0.2 ft per second are difficult to distinguish in a natural environment in which the velocities are varying in time and in space. All of these definitions are somewhat arbitrary, although they all recognize the fact that the relationship of the jet velocity to the ambient velocity is the main consideration in whether the plume is jet dominated or ambient diffusion dominated. The work to be discussed in this chapter will attempt to review the relative magnitudes of the diffusion and entrainment terms to provide some further insight into this question.

#### RELATIONSHIP OF ENTRAINMENT TO SPREADING

There are two ways which are used to formulate integral equations for jet description. One of these is the method that is used for the current report,

the entrainment description. However, an equivalent description of jet behavior can be obtained by specifying the rate at which the jet width grows. A review of such descriptions will provide insight into the relationship of these two approaches. In addition, it may be that a comparison of the relative importance of diffusion and jet mixing can be achieved more easily by a review of the spreading ratios than by consideration of the dilution rates. It is with that goal in mind that the following discussions are presented. Intermediate steps and details will be omitted in the following to enable the reader to more closely follow the broader picture. The reader is referred to the basic literature for details on the initial presentations. The equations developed herein can be verified by following the steps outlined here.

Abramovich (12) represents a basic description of the jet spreading equation. Jirka et al (10) further discussed this equation, shown here as Equation 24. As the angle  $\beta$  approaches zero, or the jet becomes aligned

$$\frac{db}{ds} = k_j \frac{1-m}{1+m} \quad (24)$$

in which  $k_j$  = jet spreading coefficient  
and  $m$  is given by Equation 25

$$m = \frac{U_a \cos \beta}{U_a \cos \beta + u_c} \quad (25)$$

with the ambient current, the Equation 24, along with Equation 25, is simplified. This yields Equation 26, a jet spreading coefficient as a function of the

$$k_j = \frac{db}{ds} \left\{ 1 + \frac{2A^*}{U_r} \right\} \quad (26)$$

in which  $A^* = U_a/U_0$   
 $U_r = u_c/u_0$

spreading ratio and pertinent physical parameters. Jirka et al report on values which have been presented in the literature for the spreading coefficient,  $k_j$ . They report results for situations where the profile is assumed Gaussian. For a three-dimensional jet, the coefficient value of 0.114 is found, while the corresponding  $k_j$  equals 0.154 appears for the two-dimensional jet. For plumes, representing discharges with pure buoyancy and no initial momentum, the values become 0.102 and 0.147 for 3 and 2-dimensional discharges respectively. These values give some measure of the expected value for this spreading coefficient.

The main point of concern in the plume is likely to be where the jet angle has become very shallow, for this would correspond to dominance by the ambient current. Therefore, as a beginning step, a comparison between the spreading ratio and the entrainment coefficient will be developed where the angle is assumed to be zero. The three equations which will be utilized will include the



conservation of mass relationship, Equation 11, the X momentum equation, Equation 13, and the expression for the change of width found by rearranging Equation 26. The detailed steps would be omitted here. However, the derivative shown in Equations 11 and 13 can be expanded. The change of the centerline excess velocity with distance can be evaluated from the expanded version of Equation 13 and substituted into the conservation of mass relationship. This enables one to find an expression for the spreading ratio,  $db/ds$ , which can then be inserted into Equation 26 to find an expression for the spreading coefficient,  $k_j$ . This results in Equation 27 which is written in terms of the excess velocity and the ambient velocity for ease in seeing their relationships, rather than in terms of the two parameters shown in Equation 26. Notice that Equation 27 becomes invalid if the ambient velocity,  $U_a$ , is zero. However, in that case, the current discussion is of no interest.

$$\frac{k_j}{E} = \frac{(2 + U_p)(1 - J)}{1 - J(1 + 0.9 U_p + 0.316 U_p^2) + 0.45 U_p} \quad (27)$$

$$\text{in which } U_p = u_c/U_a \\ J = 0.450 / (0.9 + 0.632 U_p)$$

Equation 27 represents the value of spreading coefficient at any point along the plume, as long as the angle with respect to the ambient current is not great. It is interesting to look at Equation 27 in the limit, as the excess velocity  $u_c$  reaches zero. Substitution into Equation 27 yields Equation 28, which illustrates that in the limit the coefficient would have a value of 0.10 for an E value of 0.05 which is currently suggested for the model. This is within the range of coefficients noted before based on empirical evidence. It

$$\lim_{u_c \rightarrow 0} k_j = 2E \quad (28)$$

is also worth noting that the spreading coefficient will decrease along the jet axis, approaching the value represented by Equation 28. Therefore, the average value over the length of the jet would be somewhat higher than given by Equation 28 and might very well be in the range of 0.15 for two-dimensional jets reported in earlier literature. It should be noted that those spreading ratios were determined, however, where no ambient current existed.

Solution of Equation 26 for the spreading ratio, along with substitution of Equation 27, presents an expression for the jet spreading at any point along the axis, so long as the angle is near zero.

#### SPREADING RATIO IN DIFFUSION SOLUTIONS

A number of diffusion solutions have appeared in the literature for a source of finite size. One which seems particularly useful for the current

review is the one represented Brooks (47). Brooks presents solutions for a two-dimensional diffusion problem emanating from a source of finite depth and width. He presents solutions for a variety of diffusion coefficients ranging from a constant coefficient to one which varies with the plume width to the 4/3 power. The solution which will be utilized here assumes a constant coefficient for lateral diffusion. Equation 29 presents the basic solution

$$\frac{b}{b_0} = \left(1 + 2W \frac{s}{b_0}\right)^{1/2} \quad (29)$$

in which  $b_0$  = initial plume width  $b_0$

$$W = \frac{12 D_y}{U_a b_0}$$

$D_y$  = transverse diffusion coefficient

for the width of the plume. Equation 29 can be differentiated to yield an equation for the plume spreading rate. This is shown in Equation 30. This equation could be used for direct comparison to the jet model prediction of the spreading ratio determined by combining Equations 26 and 27.

$$\frac{db}{ds} = W \left\{ 1 + W \frac{s}{b_0} \right\}^{1/2} \quad (30)$$

One item deserves additional mention with respect to Equations 29 and 30. In this particular equation the longitudinal distance  $S$  is measured from the source location. The model is developed assuming a Gaussian profile, which is different from the polynomial profiles being used in the current jet model. In addition, the width of the source here in Equations 29 and 30 represents a finite source directed downstream with the ambient current. This source width may not be the same as the physical source width associated with the jet discharge. It might therefore be necessary in some comparisons to consider the possibility that the diffusion equation should be compared with the jet equation by establishing a virtual source location ( $S = 0$ ) for the diffusion source. This would be the imaginary location where the source was presumed to be located such that the diffusion model gave comparable widths and concentrations at the point where the jet became parallel to the ambient current.

In order to use Equation 30 for estimates of the rate of growth of the plume, values need to be specified for the transverse diffusion coefficient,  $D_y$ . In river systems this coefficient is usually described in the form given by Equation 31. The value of  $\alpha$  ranges from about 0.2 for very straight,

$$D_y = \alpha H u^* \quad (31)$$

in which  $\alpha$  = dimensionless coefficient  
 $H$  = total river depth  
 $u^*$  = friction velocity of river

uniform channels up to values of two or more where a stream bend exists in a river. In fact, values as high as 10 have been reported for this parameter in very sharp bends in the Missouri River coupled with the existence of groins in the river. It is believed more likely that values of 2 or less will prevail. In most rivers which are natural, it is not likely that  $\alpha$  will be much less than about 0.4. Some authors, for example Holley et al (48) use a slightly different form of Equation 31, shown here as Equation 32. In Equation 32 the value of

$$D_y = K_d H U_a \quad (32)$$

in which  $K_d$  = dimensionless coefficient

$K_d$  usually ranges between about 0.02 and 0.06 for typical rivers. Equation 32 has an advantage for these preliminary investigations in that it simplifies the form of  $W$ . This expression can be written, using Equation 32, in the form of Equation 33. Notice that if the river depth and the discharge canal depth

$$W = 12 K_d \frac{H}{b_0} \quad (33)$$

are the same, as they are usually assumed to be for the current model, then the ratio  $H/b_0$  can be replaced by the depth-to-width ratio of the discharge canal. Insertion of Equation 33 into Equation 30 enables calculations of the jet spreading ratio as a function of the downstream distance. These calculated values can then be compared directly with the results of utilizing Equations 26 and 27 for the jet model prediction.

The relative importance of jet entrainment and ambient diffusion can be studied by comparing various results from the jet model with results using Brooks' or similar diffusion solutions. In addition, a diffusion term can be included directly in Equations 16 and 17 of the jet model. Consider Equation 16, for BOD. The basic equation must include a term on the right hand side of the equation.

$$\text{diffusion term} = \int_{-b}^{+b} \frac{\partial}{\partial \eta} D_y \frac{\partial L}{\partial \eta} d\eta \quad (34)$$

in which  $\eta$  = distance from jet axis

The polynomial expression (Equations 5 and 7) for BOD can be inserted into Equation 34 and the integration performed. This will yield the following term for the right hand side of Equation 16.

$$\text{diffusion term} = \frac{3}{2} \frac{L}{b} D_y \quad (35)$$

The coefficient  $D_y$  will be evaluated by Equation 31. This term is non-dimensionalized in the same fashion as the remainder of the equation for internal solution in the computer program.

A number of numerical tests were run using the tools outlined in the preceding paragraphs. The goal is establishment of a realistic criterion for the end of the jet region. It must be recalled that in any instance the region of jet dominated flow will be a function of the relative importance of jet entrainment and ambient turbulence. This means that the end of the jet region is not only a function of the jet characteristics but also the local stream characteristics as exemplified in a diffusion coefficient. This diffusion coefficient may vary locally, as within a bend and from one side of the river to the other. It is clear that any criterion for the end of the jet region must include as a minimum dependence on the following features:

1. Velocity ratio
2. Angle of discharge
3. Local diffusion coefficient

In addition to the velocity ratio, the absolute magnitude of the velocities involved is significant.

Several criteria were proposed and tested for defining the end of the jet region. Some were based on perceived ratios of entrainment to diffusion behavior, while others were based on simple measures of plume performance. The criteria tested included the following:

1. Determination of the relative percentages of dilution at any point due to entrainment and diffusion.
2. Determination of the point at which significant deviation from the jet results occur when diffusion is incorporated as in Equation 35.
3. Finding the point at which the jet centerline concentration decrease gradient reaches that expected from a two-dimensional diffusion source.
4. Finding the point at which the jet spreading rate becomes equivalent to that from a diffusion solution. This can be accomplished by finding at each point, an equivalent source location and width to yield the same width and peak concentration as given by the jet model and then calculating the spreading rate at that point by Equation. A simpler, but much less exact way, is to find the point at which the jet spreading rate equals the maximum from the diffusion solution, given by  $W$ , as in Equation 29.
5. The criterion offered by Jirka, et al (10) as the point at which the velocity excess,  $u_c$ , is ten percent of the initial excess.
6. A criterion based on Abramovich's (12) observation, essentially  $u_c/U_a \leq 0.10$ , or the jet velocity is less than ten percent above the ambient.

7. A further criterion that the jet influence be considered dissipated when  $u_c$  reaches some absolute minimum value, say 0.1 - 0.2 ft/sec. A review of Equation 19 indicates the strong variability of  $U_a$  throughout the cross-section of a typical stream. Hence,  $u_c$  in this range will still be much smaller than the variation of  $U_a$  throughout a typical cross section.
8. Determination of the point at which an initially perpendicular discharge is within a set angle of the ambient current, say 5 or 10 degrees.
9. A further constraint separate from the previous one is the determination of the point at which the jet strikes the bank, for the jet model is no longer applicable at that point.

Each of the criteria gives, either by itself or in combination with another one, insight into jet behavior, but no one criterion presented a simple system to use for all cases. Therefore, the presentation here will summarize the results plus show one approach which might be useful. The use of Equations 26 and 27 enables one to calculate the spreading ratio as a function of  $u_c/u_0$ . Figure 4 illustrates this for three different values of  $A = U_a/U_0$ . The values at the highest values of  $u_c/u_0$  are slightly in error, as Equations 26 and 27 assume the angle with respect to the ambient current is zero. For any given site, one can then attempt to calculate  $D_y$  based on Equation 31 and then find  $W$ , or estimate  $W$  directly from Equation 33. A look at Equation 30 shows that maximum spreading from the diffusion source occurs when  $x = 0$ . This maximum rate is then simply equal to  $W$ . As an approximation then, one could enter Figure 4 and determine the value of  $u_c/u_0$  for which the given discharge has  $db/ds = W$ . One could then go to jet model output to determine the axial location at which this value of  $u_c/u_0$  is reached. A review of other features (jet angle, absolute value of velocity excess, etc.) could then aid in deciding whether this is in fact a reasonable place to end the jet region. As an example, consider a situation where  $K_d$  in Equation 33 is estimated as 0.02, with  $H/b_0 = 0.2$ , yielding  $W = 0.048$ . In addition, consider  $K_d = 0.04$ , yielding  $W = 0.096$ , thereby doubling the influence of diffusion. Table 1 shows values of  $u_c/u_0$  found from Figure 4. Note that an interested user might have to generate other curves similar to Figure 4 for the specific values of  $A$  of interest to him. The values in Table 1 are translated into actual distances in feet for the following specific example:

$H = 4$  feet  
 $U_a = 0.6$  ft/sec  
 $\beta_0 = 90^\circ$   
 $Q_p = \text{plant discharge} = 48$  cfs

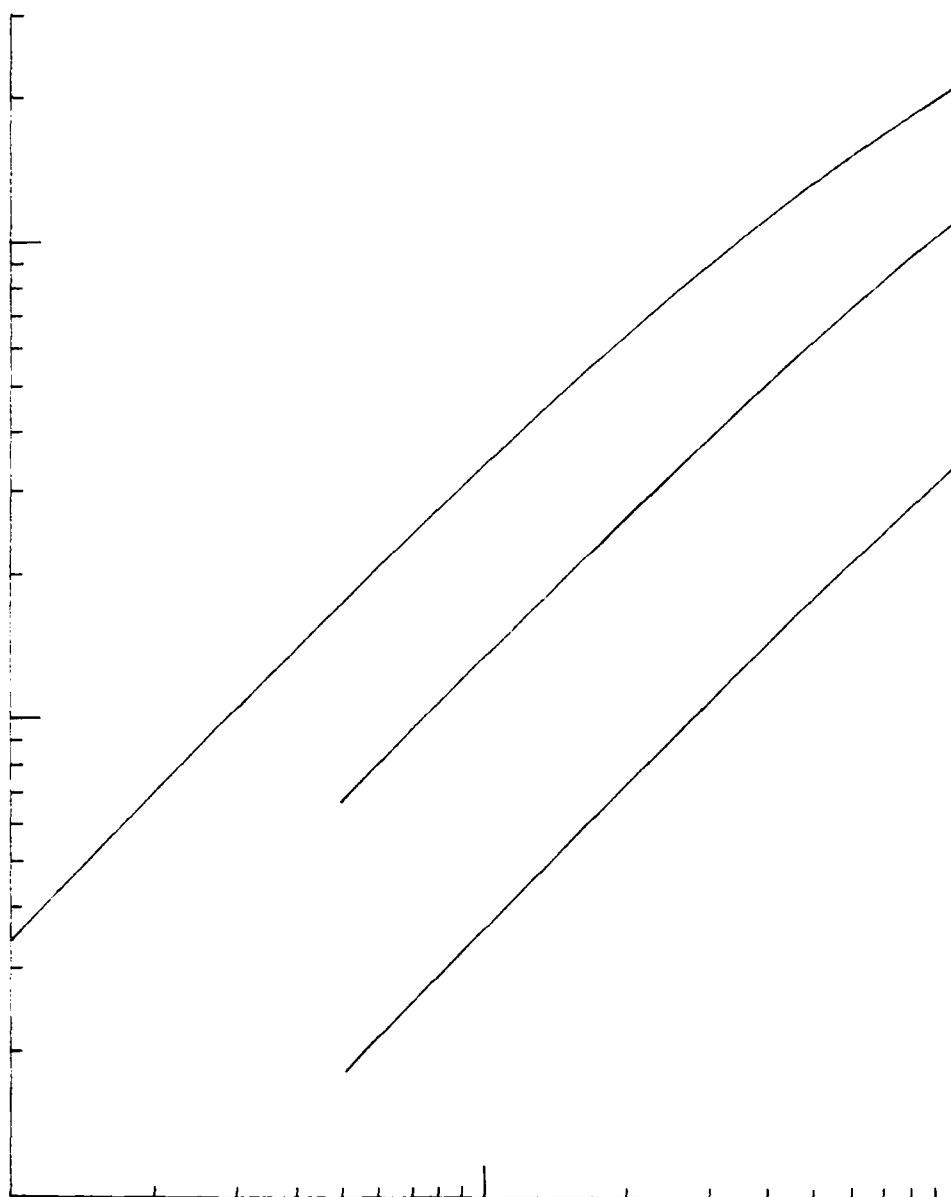


FIGURE 4 - SPREADING RATIO FROM JET MODEL

TABLE 1 - VALUES OF CUTOFF VELOCITY  
RATIO FOR EXAMPLE

A	Points defined by $db/ds = W$					
	W = 0.048			W = 0.096		
	$u_c/u_0$	$\frac{sE}{b_0}$	S'ft	$u_c/u_0$	$\frac{sE}{b_0}$	S'ft
0.8	>0.99	a	a	>0.99	a	a
0.5	0.37	0.89	290	0.81	0.1	33
0.25	0.14	9.5	1740	0.31	1.8	330

a: negligible

As expected, the strongest jet (lower A) requires a greater length to the end of the jet region. Note that for  $A = 0.8$ , the discharge could probably be analyzed as a diffusion discharge from the beginning. In fact, numerical runs by the author with 2-D diffusion models by Prakash (42) and Benedict (43) confirm this. For lower values of A, this method yields what appears to be reasonable lengths, although the 33 feet for  $A = 0.5$  and  $W = 0.096$  may be suspicious. The shortness of the lengths should not mask the dilution which occurs in these regions. For example, for  $W = 0.048$ , the dilution at the suggested cutoff point is about 1.5 for  $A = 0.5$  and over 4 for  $A = 0.25$ .

The use of the methodology presented in the example is not intended to be an absolute procedure, but rather to provide guidance in the decision-making process. Several other guidelines can be provided based on the numerical experimentation performed. These are shown in Table 2.

TABLE 2 - ADDED GUIDELINES  
FOR DEFINING END OF JET REGION

1. $u_c = 0.2$ ft/sec for $U_a$ less than 2.0 ft/sec
2. $u_c = 0.1 U_a$ for $U_a$ greater than 2.0 ft/sec
3. Cutoff $u_c/u_0$ always greater than 0.1 except for extremely high $u_0$

4. Plume angle less than 5 degrees (initially perpendicular discharge)
  5. Plume strikes near or far bank
- 

#### STATUS OF FINDINGS ON END OF JET REGION

It is clear that no very precise guidelines are available, although some quantitative guidance is provided in this report based on jet spreading ratio. Note that the type of finding exemplified by Figure 4 and Table 1 are dependent on a number of factors, including, for example, the entrainment coefficient  $E$  and the empirical relationship used to define the angle at the end of the ZOF. In addition, use of a single ambient velocity oversimplifies matters, as the lateral variation of  $U_a$  may significantly affect plume behavior. The author has observed heated water discharges which first enter a river in the lee of a bend and exhibit strong jet behavior as if into an almost stagnant ambient. However, once the plume leaves the lee region and enters the faster moving main stream, it bends rapidly downstream and looks like a diffusion situation. With all these factors considered, it is probably not reasonable to expect criteria which define the end of the jet region with extreme precision. It is believed that the criteria suggested by Table 2 and Figure 4 provide results which are consistent with findings by any of the numerical testing approaches employed. They are therefore recommended as a beginning point for further use of the model.



SECTION VI  
VERIFICATION AND SENSITIVITY  
GENERAL

Full scale verification and sensitivity testing for the existing 2-D model is probably not justified. In addition, it is not possible to find data which is adequate to verify the model components dealing with secondary components such as DO. Since some shortcomings exist due to the 2-D nature of the model along with generic difficulties in integral models (failure to account for boundaries, e.g.), the goal here will be a limited one intended to define reasonable model use and insight into expected accuracy and model sensitivity.

SENSITIVITY

Model sensitivity to various input parameters will be investigated by reporting results of numerous runs made varying one input parameter at a time. One basic **example** was selected, similar to one used by Rood and Holley (7) and taken from Velz (3). The basic data for this case are presented in Table 3.

TABLE 3 - PARAMETER VALUES FOR BASIC CASE

Parameter	Value
$U_a$ = ambient velocity	0.6 ft/sec
$H$ = ambient depth	4.0 ft
$B$ = river width	473 ft
$L_a$ = mixed river BOD	12.15 mg/l (loading of population equivalent of 311,000)
$K_1$ = deoxygenation coefficient	0.416/day
$K_2$ = reaeration coefficient	1.38/day
$L_a$ = ambient BOD	0

$D_a$ = ambient deficit	0
$Q_p$ = plant discharge	48 cfs
$L_0$ = initial BOD in discharge	200 mg/l

Items to be reviewed in assessing sensitivity include initial and ambient BOD levels, reaeration ( $k_2$ ) and deoxygenation ( $K_1$ ) coefficients, settling coefficient ( $K_3$ ), and velocity ratio ( $A$ ) and initial angle. In addition, some of the basic jet model parameters, such as the entrainment coefficient ( $E$ ) and the drag coefficient ( $C_D$ ) will be varied to observe the influence. As noted, a full scale sensitivity analysis is not contemplated here. Instead, the impact of each parameter will be discussed relative to its importance for the models' use as a planning and assessment tool.

In reviewing the apparent impact of any parameter, discussions in Section V should be kept in mind. The only significant impact is that expected to occur within the jet region as defined by some cutoff criterion. Seemingly significant changes which occur at further distances downstream are not important, for the jet model really should not be used at those distances.

#### ENTRAINMENT COEFFICIENT

An internal parameter of major importance in the model is the entrainment coefficient,  $E$ , which is currently used as 0.05. As the degree of jet entrainment is proportional to the value selected for  $E$ , its impact may be considerable. On the other hand, it is not desirable to have to specify a different value of  $E$  for each case, due to the probable difficulty of relating this parameter to environmental conditions. It is believed that 0.05 is a reasonable value, but its impact should be reviewed. Table 4 shows results of some runs made with  $E = 0.025$ , 0.050, and 0.100, with other values as shown in Table 3.

TABLE 4 - SOME RESULTS OF  
VARYING THE ENTRAINMENT COEFFICIENT

$S/b_0$	$E = 0.025$		$E = 0.050$		$E = 0.100$	
	DOD, mg/l	BOD, mg/l	DOD, mg/l	BOD, mg/l	DOD, mg/l	BOD, mg/l
40	0.16	109.8	0.14	85.9	0.12	66.1
100	0.33	80.8	0.28	6.12	0.24	46.5
200	0.54	60.3	0.46	45.6	<u>0.38</u>	<u>35.6</u>
300	0.73	50.3	0.59	47.8		
400	0.84	43.8	<u>0.70</u>	<u>32.9</u>		
600	1.07	35.8				
800	1.26	30.9				

In Table 4, DOD implies dissolved oxygen deficit. The different number of entries represents the different points at which  $u_c/u_0 = 0.10$  is reached. Note this occurs much earlier for  $E = 0.10$ , which is expected. Note that it takes about three times the downstream distance to dilute the effluent to about 35.8 mg/l if  $E$  drops from 0.10 to 0.025. The distance is approximately doubled when  $E$  drops from 0.05 to 0.025. It is apparent that the entrainment coefficient value has a major impact, but further considerations will have to await attempts to verify the model against data.

#### DRAW COEFFICIENT, $C_d$

Another parameter included in the jet model proper is the drag coefficient,  $C_d$ . A value of 0.5 has been selected based on work by Motz and Benedict (14). For comparison, the standard run was made with  $E=0.05$  and values of  $C_d = 0.1, 0.5$ , and 1.0. Generally, at corresponding distances downstream, higher values of  $C_d$  yielded slightly lower DOD values and BOD values, but very small differences were noted. For example, at  $s/b_0 = 300$ , changing  $C_d$  from 0.1 to 1.0 changed the DOD from 0.64 to 0.56 mg/l, while the BOD changed only from 39.3 to 36.4. Therefore, in terms of dilution, changes in  $C_d$  have little impact. The major effect of  $C_d$  comes in predictions of trajectory. One measure of this is  $y_{max}/b_0$ , the dimensionless value for the centerline distance away from the near shore when it becomes parallel to the ambient current. Table 5 shows this variation, along with the length to  $u_c/u_0 = 0.10$ .

TABLE 5 - RESULTS OF VARYING DRAG COEFFICIENT

Parameter	$C_d = 0.1$	$C_d = 0.5$	$C_d = 1.0$
$y_{max} / b_0$	218	46.7	24.0
$S/b_0$ at which $u_c/u_0 = 0.10$	270	406	470

It is clear that the biggest difference in results occurs when  $C_d$  is dropped to 0.1. It appears that values for  $C_d$  in the range of 0.5 - 1.0 are much more reasonable. Many workers have found that failure to include a reasonable drag value gives quite erroneous behavior. Until further findings develop from verification attempts. e.g.,  $C_d$  will be retained at its current value of 0.5.

#### ANGLE AT END OF ZONE, $\beta_0$

The current source of  $\beta_0$  is the empirical evidence accumulated by Motz and Benedict (14) showing the angle as a function  $A$  of the velocity ratio. There is a degree of scatter in the data, as expected. Therefore, it was decided to check model sensitivity to the exact value selected. The value determined from the Motz-Benedict data was varied both plus and minus an increment. The specific runs used  $A = 0.25$ , where the standard  $\beta_0 = 65^\circ$ . Values of  $\beta_0 = 56^\circ$  and  $74^\circ$  were used for comparison. In addition, values of  $E = 0.05$  and 0.025 were used. Table 6 and 7 show important findings from these runs.

TABLE 6 - GENERAL PLUME COMPARISONS  
FOR VARIATION OF INITIAL ANGLE

Parameter	$\beta_0 = 56^\circ$		$\beta_0 = 74^\circ$	
	E = 0.025	E = 0.050	E = 0.025	E = 0.050
$Y_{\max} / b_0$	43.4	42.6	51.6	49.9
$s/b_0$ for $u_c/u_0 = 0.10$	1124	510	768	310

TABLE 7 - DILUTION COMPARISONS FOR  
VARIATION OF INITIAL ANGLE (E = 0.05)

$S/b_0$	$\beta_0 = 56^\circ$		$\beta_0 = 74^\circ$	
	DOD, mg/l	BOD, mg/l	DOD, mg/l	BOD, mg/l
20	0.07	107.9	0.09	106.7
40	0.14	85.4	0.15	86.5
100	0.26	60.0	0.31	61.8
200	0.41	44.2	0.51	47.3
300	0.54	36.5	0.65	39.4
500	0.73	28.4		

In comparing with these results, values for the standard angle of  $65^\circ$  can be found in Table 4 and Table 5. Values comparable to those in Table 7 but for  $E = 0.025$  give differences similar in magnitude to those found in Table 4 and will not be presented here. It is important to observe that the 18 degree range used here is rather large and should encompass any likely value. Despite this large range, the changes due to variation of  $\beta_0$  are much smaller than those due to changes in  $E$ . This is especially true if one looks at the dilution of BOD, which is the prime indicator of mixing processes here. Differences in BOD at the respective points are negligible. The main conclusion here seems to be that the value for  $\beta_0$  found from the Motz-Benedict data is completely satisfactory within the ranges of accuracy needed.

#### AMBIENT BOD: $L_a$

Runs to this point have all used  $L_a = 0$ , or zero BOD found in the water arriving from upstream. In natural environments,  $L_a$  may of course be greater than zero due to upstream sources, either natural or manmade, of BOD. The impact of  $L_a$  was tested by using two different values ( $L_a = 1$  and  $L_a = 5$  mg/l) with the run for which  $A = 0.25$ ,  $\beta_0 = 650$ ,  $E = 0.05$ . Results from this example are included in Table 4 and Table 5. In these runs, since nothing changes to alter jet hydrodynamics, the velocity and width variation, as well as plume trajectory remain the same. However, the added stream BOD causes somewhat greater downstream concentrations. For example, at  $s/b_0 = 400$ , values of BOD are 31.6 and 32.8 mg/l for  $L_a = 1$  and 5 mg/l, respectively. Corresponding values of DOD are 0.71 and 0.83 mg/l. In short, the value of  $L_a$  probably does not have to be specified with great accuracy if the discharge concentration is sufficiently high. It should be recognized that if  $L_0$  is low enough, however, then the ambient value is a dominant factor and can not be neglected.

#### SEDIMENTATION COEFFICIENT, $K_3$

Runs to look at the value of  $k_3$  were made using a river width of 197 feet and a reaeration coefficient,  $k_2$ , of 0.138/day. This is one-tenth the value of  $k_2$  used for other runs. The purpose of this changes is to maximize the likely impact of  $K_3$ . For comparison with the no settling ( $k_3 = 0$ ) case, a run was made with  $K_3 = 0.416$ /day, the same value as  $K_1$ . This run and some made with  $K_1 = K_2 = 0$  show a major feature of plume behavior. By far the greatest reduction in BOD (or any other similar constituent) occurs by dilution, rather than by any sort of decay. For instance, the increase of  $K_3$  lowered BOD at  $s/b_0 = 500$  only from 74.2 mg/l to 71.7. The deficit at this point changed from 2.61 to 2.57 mg/l, a negligible amount. Notice how much greater these deficits are than those reported in earlier tables. This is due to the much lower value for  $K_2$ . These findings and others not shown here suggest that no factors are as important as the basic jet description in the jet region. Downstream from the end of the jet region, sufficient time exists for rate coefficients to have some effect. Upstream, in the jet region, exact specification of the rate coefficients is really not necessary; especially  $K_1$  and  $K_3$  are over shadowed by dilution. Wide variations in  $K_2$  will have greater impact.

#### REVIEW OF SENSITIVITY FINDINGS

No results have been explicitly reported here for the variation of initial discharge angle ( $\beta_0$  in Figure 1) or velocity ratio  $A$ . Preliminary results have been presented in Reference 1 and some portions will be reviewed in a later example. Trends are what would be expected. Discharges which are more clearly jets (low values of  $A$ ) provide quickest early mixing and smallest DO deficits. Discharges with low  $A$  values are more apt to perform poorly.

Probably the single most critical observation is that the primary reduction of BOD occurs by dilution, not decay, in the jet region. Therefore, the input to the jet region should focus more on description of jet behavior than on chemical

and biological dynamics. This assumes that reaction rates are similar to those expected for organic wastes. Obviously, if some immediate and large uptake occurred, this would be an important part.

#### VERIFICATION

The primary data to be used for model verification is some data collected by Carter, et al (16). Several of their runs were distinctly two-dimensional initially. Unfortunately, their discharges were buoyant. Therefore, it may be expected that some observed spreading rates will be greater than accounted for by the current model. However, it is believed that this in itself will be useful in defining limits of model applicability.

Table 8 shows the data for the basic Carter runs to be analyzed herein.

TABLE 8 - DATA FROM TWO-DIMENSIONAL  
RUNS BY CARTER, ET AL (16)

Run	$h_0$ ft	$H$ ft	$B_0$ ft	$Ar = h_0/B_0$	$U_0$ ft/sec	$U_a$ ft/sec	$R = 1/A$	$F_j$
A	0.174	0.167	0.163	1.07	0.31	0.18	1.75	3.50
B	0.174	0.167	0.065	2.68	9.79	0.18	4.38	8.92
C	0.174	0.167	0.0325	5.35	1.58	0.18	8.78	17.78
D	0.174	0.167	0.0812	2.14	0.32	0.18	1.80	3.65
E	0.174	0.167	0.0325	5.35	0.79	0.18	4.37	8.86
F	0.174	0.167	0.0163	10.71	1.58	0.18	8.81	17.86
G-II	0.179	0.168	0.065	2.75	0.77	0.18	4.26	8.38
H-II	0.185	0.167	0.043	4.35	1.14	0.18	6.32	12.43
J-II	0.178	0.168	0.146	1.22	0.34	0.18	1.91	3.80

Note:  $F_j$  = densimetric Froude number

In looking at Table 8, runs most likely to present difficulties are runs A, D, and J-II. All three of these have a low value of  $R$  (high  $A$ ) and a fairly low densimetric Froude number, implying importance of ambient diffusion and buoyancy-generated lateral currents, respectively. In addition, note that the discharge channel aspect ratio,  $Ar$  (depth/width) is unfortunately not in a very practical range. Most discharge channels tend to be wider than they are deep with  $Ar$  values approaching 0.1-0.2 or even lower. This will likely have the effect of enhancing the effect of buoyancy relative to entrainment because

it might enable the entire plume to lift off the channel bottom due to buoyancy and become in effect a three-dimensional discharge despite its two-dimensional beginnings. The total effect of these factors may cause the plume to exhibit more rapid lateral growth and dilution than predicted by the current model.

#### CENTERLINE TEMPERATURE DECREASE

A very important characteristic of any effluent plume is its axial decrease of concentration. Runs were made for all nine runs outlined in Table 8. Figure 3 shows results, with Carter's data plotted and model output shown.

Figure 5 illustrates typical findings from the runs. In reviewing this and later figures, the scatter of the data must be kept in mind. Generally runs A and C are well represented by the model. The exception is in the later points, where the data falls off much more rapidly than shown by the model. It appears that by this point ambient turbulence has begun to play a major role and therefore dilution will be occurring at a faster rate than shown by the jet model alone. It is interesting to note that use of Figure 4, with  $W = .048$ , by interpolation yields a cutoff  $u_c/u_0$  of about 0.25. This is almost identically the point at which the results begin to fall below the jet model predictions.

Runs B and H-II do not seem to fit so well. The dotted curve on Figure 5 is the model curve for Run H-II moved so that the end of the ZOFE corresponds to the data of Carter, et al (16). The solid curves are all based on the Motz-Benedict (14) data. Notice that when this adjustment is made, then the model does a good job of representing the data. Once again, the data begins to fall off more rapidly when ambient diffusion becomes important. Similar agreement can be obtained by shifting Run B. It appears that the ZOFE data by Carter and Motz-Benedict may be at odds. A major difference in the two sets of data lies in the relative depth of the receiving waters. Carter's work used here had the discharge filling the entire receiving channel depth, while Motz and Benedict used discharges covering only a small portion of the receiving water depth. Evidently, some difference in behavior results, although it does not appear to affect the higher jet velocities ( $R = 8.78$ ).

Data for the other runs shown in Table 8 are not presented here, for they reinforce the findings presented. They actually enhance model verification by illustrating the data scatter more. In summary, the model proper seems to do a good job of predicting near-field behavior up to the point where ambient turbulence is important. However, this verification step has pointed out the need to better define the point where the ZOFE ends and hence the model begins.

#### LATERAL VARIATION OF CONSTITUENTS

The polynomial forms selected for lateral variation of constituents were verified by plotting against Carter's data. An example of one run is shown in Figure 6. The parameter  $n_{1/2}$  is the lateral distance (measured from the jet axis) to the point at which the concentration is one-half the centerline value.

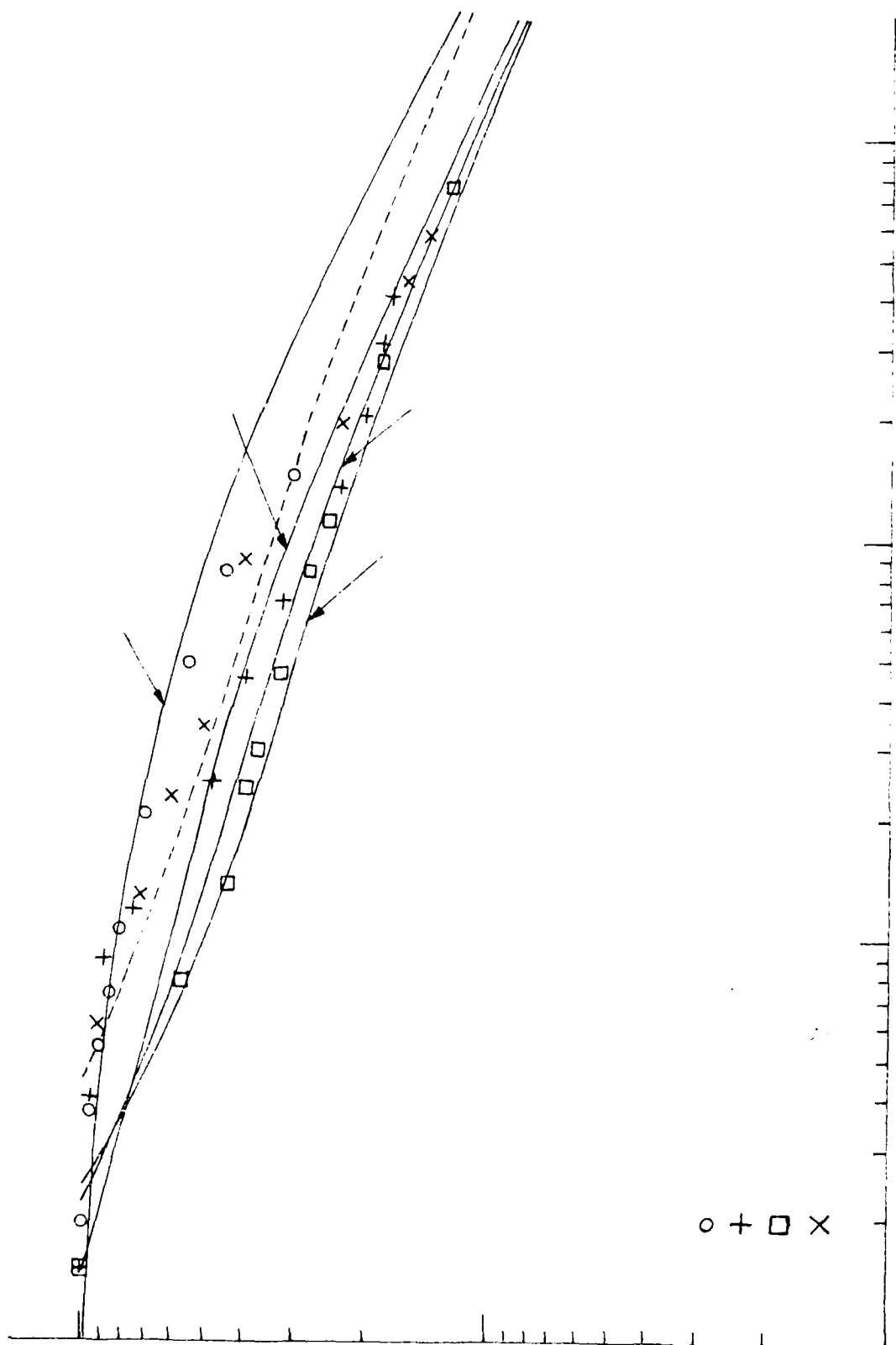


FIGURE 5 - CENTERLINE TEMPERATURE DECREASE



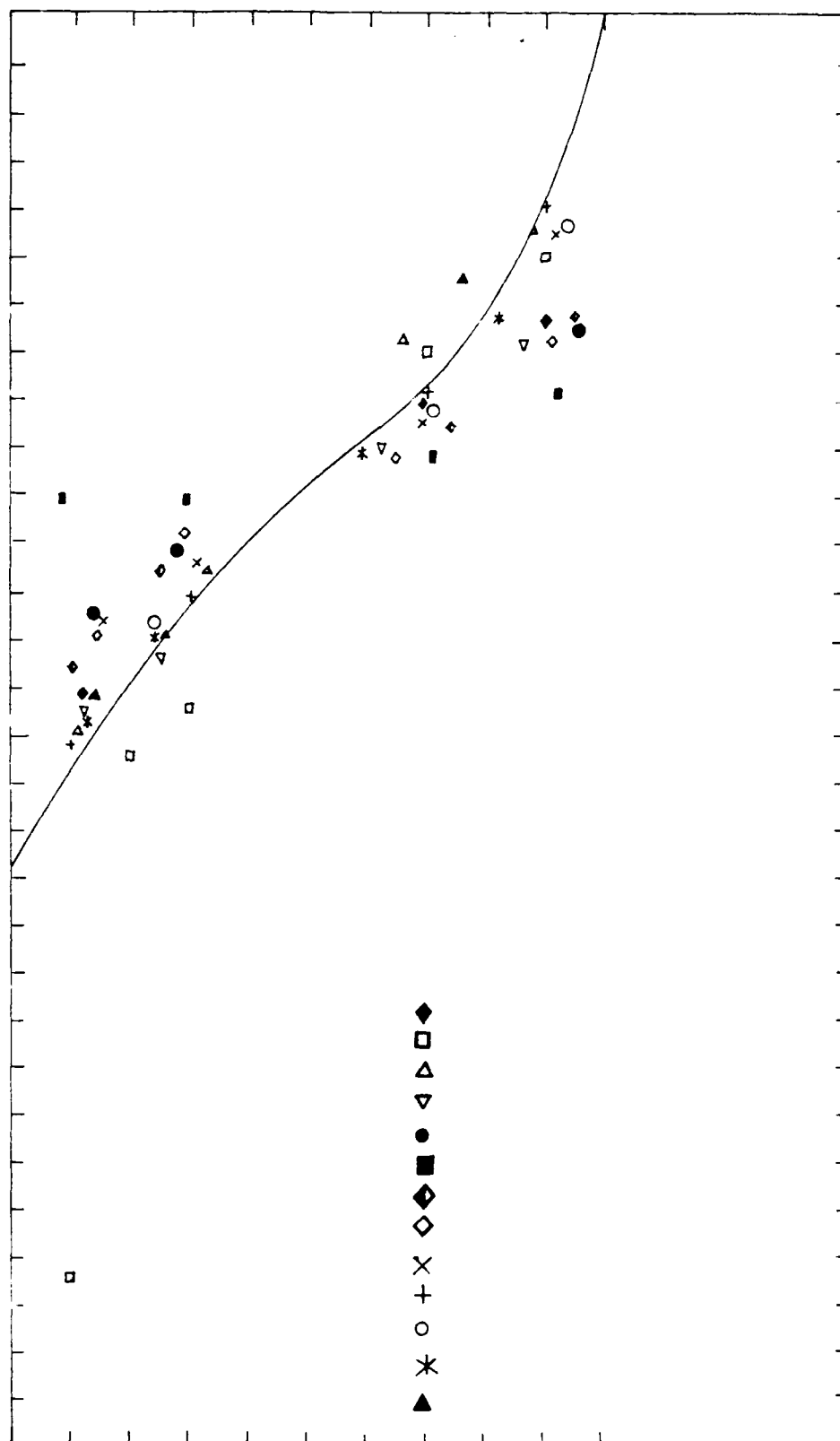


FIGURE 6 - LATERAL VARIATION OF CONCENTRATION

The solid line curve fits the data adequately, although the scatter is so great that a Gaussian curve, a cosine curve presented by Carter, et al (16), or any of a number of similar curves could have been used as well. Even though the data scatter prevents a definitive statement, it seems clear that the polynomial chosen gives an adequate representation.

#### VARIATION OF PLUME WIDTH

Carter, et al (16) present data on plume width for Runs A, B, and C. It is presented in reduced form as a graph of width versus axial distance. Attempts were made to use the model output for comparison to this data. Obviously, however, some problem exists, for model widths were all substantially less than data. While this might be expected in later regions due to ambient diffusion, the dilution fit shown in Figure 5 suggests that the basic plume dimensions should be similar. A careful review of Carter's data indicated that the major problem again appears to involve definition of properties at the end of the ZOFÉ, in this case the width. If the widths shown by Carter's data are used, then the model output agrees well with data. On the other hand, if the width shown by Equation 23 is used, the values from the model are too small. Here, some discrepancy may exist, for Carter's reported data suggests abnormally large widths at the end of the ZOFÉ, as much as 3-5 times the values given by Equation 23. While this equation is theoretical only, it is believed to provide reasonable widths based on other data. Carter's data suggests that plume width grows by a factor of 4-10 within a downstream distance of only 2-3 widths. This seems unlikely. However, the raw data were not available for resolution of this question. Therefore, no figure will be presented. It can be stated that the model predicts the trend of width growth well, but some discrepancy exists concerning the width at the end of the ZOFÉ. Future work should attempt to resolve this problem.

#### GENERAL ON VERIFICATION

The verification against the data by Carter, et al (16) has shown the model to be a very good model for the data used. Exceptions are primarily two. First, once ambient turbulence becomes important, the model begins to under predict concentrations. Second, some questions were raised about conditions specified at the end of the ZOFÉ. In addition, runs not shown here tested the model on some of Carter's three-dimensional data and generally found that the model, as expected, did not perform as well under those conditions.

#### EXAMPLE OF MODEL UTILITY

To illustrate expected behavior and to show comparisons of the jet results to other models, several runs were made for the data shown in Table 3. The jet model was used. In addition, the finite source model defined by Equation 20 was employed, as well as the stream tube model presented by Caro-Cordero and Sayre (22).

The two jet runs show in Figure 7 both represent discharge channels perpendicular to the river. In case J1, the ratio of the ambient to discharge velocity is 0.5, while the discharge channel width is 4.4 m. In case J2, the

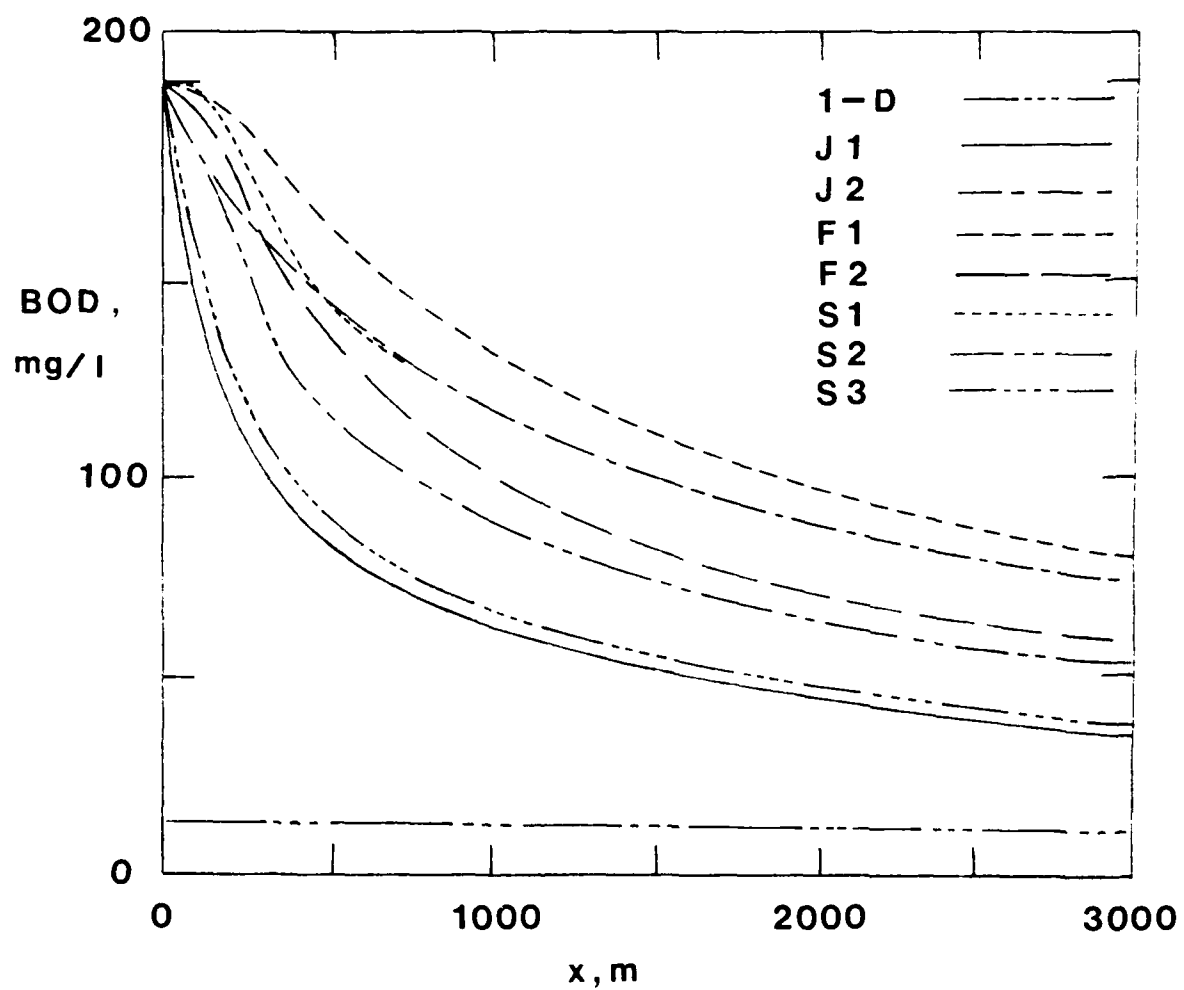


FIGURE 7 - EFFECT OF DISCHARGE MODE ON BOD

velocity ratio is 0.8, with a channel width of 7.0 m. The finite source and stream tube discharges were both assumed to be up against the bank. For the finite source case F1,  $D_y = 0.00446 \text{ m}^2/\text{sec}$ , while for F2,  $D_y = 0.00892 \text{ m}^2/\text{sec}$ . The size is selected to pass the entire BOD loading with no initial dilution. The stream tube results are also based on assuming zero initial dilution, with runs S1 and S2 using the same  $D_y$  values shown for F1 and F2, respectively. Run S3 uses  $D_y = 0.01338 \text{ m}^2/\text{sec}$ .

Several features are evident in reviewing Figure 7. First, the higher velocity jet (J1) mixes the material better and represents a distinct improvement over J2, the discharge at near stream velocity. Second, eventually, after early dilution effects are removed, all are undergoing further dilution at very similar rates. Third, it is interesting to note that especially the stream tube model gives essentially the same behavior as the jet model if a proper coefficient value is selected. Even the higher velocity jet is well-matched. It is clear that both the means of discharge and the ambient flow field makes a significant impact on the downstream BOD distribution.

Of course, the changes in BOD shown in Figure 7 are primarily due to dilution. The deoxygenation processes represented by  $K_1$  require time to proceed. This effect can be seen by reviewing the critical deficit predicted by the various methods. For both jet runs, the 1-D standard oxygen sag equation yields a critical deficit of 2.18 mg/l, while Rood and Holley (7) show a value of 9.55 mg/l. However, jet run J1 yields a value of 3.12 mg/l and run J2 a value of 6.96 mg/l for this critical deficit. In all cases it was assumed no upstream BOD or DO deficit existed. It is clear that the jet discharge J1 achieves more rapid early dilution, reducing the driving force for oxygen use, and hence the deficit. However, where the jet is not as strong (J2) the deficit is much higher, approaching that for pure diffusion. Hence, a change in the discharge can exert a considerable impact on the DO distribution downstream.

## SECTION VII

### SUMMARY OF FINDINGS AND RECOMMENDED WORK

#### APPLICABILITY OF MODEL

The model has been shown to be capable of describing near-field behavior of effluents where the situation is dominated by jet mixing and reasonably two-dimensional mixing exists. Verification against data given by Carter, et al (16) is good and demonstrates the models' utility and reliability. It can currently be employed as a planning and assessment tool for water quality studies. It may be used by itself or provide input to a larger effort using a diffusion model to carry results downstream.

The model provides an ability to assess localized impacts in excess of that shown by the usual one-dimensional models. One-dimensional conditions may not exist in the receiving water for many miles. As the one-dimensional model uses essentially a cross-sectionally averaged value of the concentration, it is clear that local regions with higher concentrations will be masked.

Several primary limitations of the model have been identified. These can be briefly summarized as follows:

1. The model is two-dimensional, thereby being invalid for cases where vertical mixing is significant. On the other hand, discharges into fairly shallow streams can be handled well by this model.
2. The model does not account explicitly for the existence of solid boundaries.
3. The model may become invalid before the one-dimensional region is reached, necessitating use of a diffusion model to carry the calculations further downstream.
4. The model does not include effects of density differences, which causes it to yield some error when dealing with highly buoyant discharges.

Despite these shortcomings, the model is believed to be a valuable tool for planning and assessment in its current form.

#### RECOMMENDED WORK

##### EXTENSION OF MODEL TO THREE DIMENSIONS

Work undertaken in the mini-grant indicates that the single biggest shortcoming of the model is its inability to predict three-dimensional behavior of a constituent plume due to the assumed two-dimensional character of the discharge. Extension of the model to three dimensions will increase the complexity of the model and the number of differential equations which must be solved, but the increase in predictive capabilities for the model will be substantial.

The best modeling of these surface discharges has been in the area of thermal plumes. Reviews by Benedict, et al (9), and Jirka, et al (10) give information on available models and the modeling techniques. Essentially, similarity profiles for velocity, density, and any constituents of interest must be assumed in the vertical direction, as well as in the lateral direction. Appropriate assumptions must also be made concerning the relative rates of entrainment in the two directions. If a three-dimensional model is going to have full utility, it should include the effect of buoyant forces. There are a number of models currently utilized widely for analysis of thermal discharges. One common model is the Prych-Davis Shirazi (PDS) model (35) which has been verified probably more fully than any other currently available model. It must still be noted that even this model has a number of shortcomings. A review of these models should be the first step in determining whether any of the models could be utilized in their basic format, with additional equations and slight modifications added to handle other constituents. Since no one model is totally satisfactory, it is likely that additional modification will have to take place. This will essentially be a process of taking the current two-dimensional model and upgrading it to the third dimension, using consistent forms for the assumed similar profiles.

In the process of extending the model to three dimensions, the method of handling the zone of flow establishment should be reviewed. The current means of handling it is purely on the basis of empirical evidence. This requires another input to the model as it is currently used, and this in turn requires some judgement on the part of the person applying the model. In order to avoid this problem, it would be good to have the zone of flow establishment characteristics solved on the computer directly, perhaps in the fashion developed by Stolzenbach et al (13). One of the major criticisms of the PDS model is its rather arbitrary way of handling the zone of flow establishment. The goal of this is not to provide a fancy analytical treatment, but to provide a useful description of the zone of flow establishment, consistent with available empirical evidence, and minimizing the required judgement on the part of those people who will ultimately be applying the model. It is believed that this can be done in a convenient fashion.

Extension of the model to three dimensions will greatly enhance its utility. This is not a matter of starting over, for all of the information garnered from the application of the two-dimensional model can be employed in the development of the three-dimensional version.

#### INCLUSION OF BOUNDARY EFFECTS

Probably the most difficult changes required in the model are those associated with the effects of the influences of lateral and bottom boundaries. It is clear that these boundaries cause significant changes in plume behavior from that which would occur in an unbounded medium. The boundaries exert a force and therefore influence the trajectory of the plume, as well as decelerating it due to boundary friction. The mixing characteristics of the plume are also changed considerably, as the existence of solid boundaries limit the amount of water available for dilution and also promote reentrainment of fluid previously entrained into the plume. This reentrainment occurs in regions where fluid is

trapped between the plume and the boundary. All of these effects are very difficult to describe in equation form and are very much dependent upon the site, for each individual section of river, estuary, or lake has its own particular bottom topography and longitudinal alignment. Therefore, it is not expected that a complete and totally general equation set can be written to completely handle the boundary problem.

By the very nature of an integral model for the jet phenomenon it is difficult to incorporate boundary influences, for the flow problem has already been reduced to one dimensional by the lateral (and vertical in the three-dimensional case) integration of the equations.

There are two categories of problems which can be identified and treated separately as far as the effect of boundary influences. The first of these is the case where the plume reaches the boundary and still contains a significant excess velocity and/or angle with respect to the ambient velocity field. The second case is the situation where the plume has aligned itself essentially with the ambient flow field and has velocities which differ by only a small percentage from the ambient velocities. These two will be discussed as to possible solutions identified in the minigrant work in separate paragraphs here.

The case where significant momentum remains in a jet when it strikes the boundary is a very difficult one to handle analytically. The two most logical approaches appear to be either adjustment of the predictions by use of empirical evidence or use of a simplified method of images approach. Wu (34) used a method of images approach in his dissertation for a jet discharge. The use of this method is not theoretically completely justified in this case because of nonlinear terms which appear in the equation. However, it may have some utility in this case, even though the predicted jet characteristics are not identical to those observed by workers treating the so-called wall jet. The state of the art is such that even an ability to predict the gross behavior of a jet which interacts with a boundary would be a major improvement. A second way in which the equations might be modified to attempt direct analytical inclusion of the boundary effects would be the methods offered by Adams (20) to include boundary influences and reentrainment of fluid trapped between the plume and the near shore. Adams' method offers theoretical advantages over the system purposed by Wu, but it has the disadvantage that an average concentration and velocity have been assumed over each cross section, rather than some profile shape. It may, however, be possible to modify Adams' work to include a representative profile shape or at least to be able to take the predicted average concentration across the section and translate it into a lateral variation of concentration.

If these analytical techniques do not appear to provide a useable tool, they might be replaced by empirical relationships which indicate the influences of boundaries. It appears now that the most likely solution to this category of problem would be some combination of the analytical treatment coupled with empirical evidence. It is unrealistic to believe that current knowledge would allow for a completely generalized solution in detail.

The second category of problems is one in which the jet is almost completely assimilated with the ambient field as far as the dynamics is concerned. That is, ambient turbulent diffusion is probably either the dominant mechanism of mixing or almost so. It seems that a proper way to handle this is to attach a diffusion model to the end of the jet region, with proper care for conservation of mass at the point where two models are connected. Due to the linear character of the diffusion equation, it is very easy to incorporate the boundary influences through use of the method of images in analytical methods or by finite differences techniques. The most general sort of diffusion model to be attached to the jet model would allow for inclusion of the effects of bends in the river and varying depths across the river.

#### SOURCES AND SINKS

One of the first steps in determining which other constituents and the proper sources and sinks to be considered in further handling of the model would be to identify specific chemicals of interest to the Air Force. All available information on the behavior of these chemicals could be determined from literature and communications with those people in the Air Force knowledgeable in the behavior of these chemicals. Attempts could be made to define appropriate rate constants for these sources and sinks for inclusion in the model. If the waste streams of interest include other pairs, such as the DO-BOD combination, which interact with each other, appropriate feedback loops could be provided in the equations. In addition, if there are materials which appear to have a decay rate which is variable according to surrounding conditions, attempts could be made to incorporate this into the model as well. For example, some substances are known to have an immediate oxygen consumption followed by a more gradual useage of oxygen.

#### NON-UNIFORM SYSTEMS

The primary non-uniformities of concern here are the variations of depth and velocity as one moves across the stream at any location, as well as the same changes moving downstream. If the ambient velocity used for the input to the jet model is assumed to be a uniform velocity, very bad results may be obtained if the real field situation has velocities which differ considerably from this average velocity. For example, frequently velocities very near the shore are considerably reduced below the main velocity, with the velocity rising to its peak some place out into the river. If the size of the plume is not large with respect to the river, much of its early jet mixing may be taken place in a region where the velocity is substantially reduced below the average stream velocity. Therefore, it would be more appropriate to use a velocity representative of the regions in which the jet mixing is actually occurring.



## CONCLUSIONS

This report outlines further development of a model originally presented in Reference 1. The current model has been shown to have limitations but to provide very useful capabilities for near-field analysis of effluent discharges. The model might be used to assess the impact of an existing discharge or to evaluate the effectiveness of possible discharge modes for a proposed discharge. It provides an ability to adjust designs not currently provided by one-dimensional models.

## REFERENCES

1. Benedict, B.A., "A Near Field Model for Dissolved Oxygen and Other Water Quality Parameters", Completion Report, ASEE-USAF Summer Program, Tyndall AFB, FL, August, 1976.
2. Dobbins, W.E. "BOD Oxygen Relationships in Streams," Journal of the Sanitary Engineering Division, ASCE, 90, SA3, June 1964, pp 53-78.
3. Velz, C.J., Applied Stream Sanitation, Wiley-Interscience, New York, 1979 619 pp.
4. Nemerow, N.L., Liquid Wastes of Industry - Theories, Practices and Treatment, Addison-Wesley Publishing Co., Reading MA, 1971
5. Holley, E.R., J. Siemons, and G. Abraham, "Some Aspects of Analyzing Transverse Diffusion in Rivers," Journal of Hydraulic Research, 10, 1, 1972, pp 27-57.
6. Ward, P.R.B., "Prediction of Mixing Lengths for River Flow Gaging", Journal of the Hydraulics Division, ASCE, 99, HY7, Jul 1973, pp 1069-1081.
7. Rood, O.E., Jr., and E.R. Holley, "Critical Oxygen Deficit for Bank Outfall", Journal of the Environmental Engineering Division, ASCE, 100, EE3, Jun 1974, pp 661-678.
8. Benedict, B.A., E.M. Polk, Jr., E.L. Yandell, Jr., and F.L. Parker, "Surface Jet and Diffusion Models for Discharge of Heated Water," Proceedings, Fourteenth Congress, International Association for Hydraulic Research, Paris, September 1971, Vol 1, Paper A22, pp 183-190.
9. Benedict, B.A., J.L. Anderson, and E.L. Yandell, Jr., Analytical Modeling of Thermal Discharges: A Review of the Art, ANL/ES-18, Argonne National Laboratory, April 1974, 321 pp.
10. Jirka, G.H., G. Abraham, and D.R.F. Harleman, "An Assessment of Techniques for Hydrothermal Prediction," Report No. 203, Ralph M. Parsons Laboratory, Massachusetts Institute of Technology, July 1975, 403 pp.
11. Morton, B.R., "On a Momentum-Mass Flux Diagram for Turbulent Jets, Plumes, and Wakes," Journal of Fluid Mechanics, 10, 1961, pp 101-112.
12. Abramovich, G.N., The Theory of Turbulent Jets, The M.I.T. Press, Massachusetts Institute of Technology, 1963.
13. Stolzenbach, K.D., and D.R.F. Harleman, "An Analytical and Experimental Investigation of Surface Discharges of Heated Water," R.M. Parsons Laboratory Report No. 135, Massachusetts Institute of Technology, 1971.
14. Motz, L.H., and B.A. Benedict, "Surface Jet Model for Heated Discharges," Journal of the Hydraulics Division, ASCE, 98, HY1, Jan 1972, pp 181-199.

15. Fan, L.N., "Turbulent Buoyant Jets into Stratified or Flowing Ambient Fluids," Technical Report No. KHL-R-15, W.M. Keck, Laboratory of Hydraulics and Water Resources, California Institute of Technology, Pasadena, California, June 1967.
16. Carter, H.H., E.W. Schiemer, and R. Regier, "The Buoyant Surface Jet Discharging Normal to an Ambient Flow of Various Depths," Technical Report 81, Chesapeake Bay Institute, February, 1973.
17. Sawyer, R.A., "The Flow Due to a Two-Dimensional Jet Issuing Parallel to a Flat Plate," Journal of Fluid Mechanics, Vol. 9, 1960.
18. Sawyer, R.A., "Two-Dimensional Reattaching Jet Flows Including the Effect of Curvature on Entrainment," Journal of Fluid Mechanics, Vol. 17, 1963.
19. Maxwell, W.H.C., and H. Pazwash, "Boundary Effects on Jet Flow Patterns Related to Water Quality and Pollution Problems," Report No. 28, University of Illinois Water Resources Center, January, 1970.
20. Adams, E.E., K.D. Stolzenbach, and D.R.F. Harleman, "Near and Far Field Analysis of Buoyant Surface Discharges into Large Bodies of Water," Report No. 205, Ralph M. Parsons Laboratory, Massachusetts Institute of Technology, August, 1975, 267 pp.
21. Liseth, P., "Mixing of Merging Buoyant Jets from A Manifold in Stagnant Receiving Water of Uniform Density," Hydraulic Engineering Laboratory, University of California, Berkeley, Report No. HEL 23-1, 1970.
22. Caro-Cordero, R., and W.W. Sayre, "Mixing of Power Plant Heated Effluents with the Missouri River," Iowa Institute of Hydraulic Research, Report No. 203, University of Iowa, Iowa City, Iowa, June, 1977.
23. Paily, P.P., and W.W. Sayre, "Model for Shore-Attached Thermal Plumes in Rivers," Journal of the Hydraulics Division, American Society of Civil Engineers, 104, No. HY5, May, 1978, pp. 709-723.
24. Rajaratnam, N., "Plane Turbulent Compound Wall Jets," Journal of Hydraulic Research, Vol. 10, No. 2, 1972, pp. 189-203.
25. Beltaos, S., and N. Rajaratnam, "Plane Turbulent Impinging Jets," Journal of Hydraulic Research, Vol. 11, No. 1, 1973, pp. 29-59.
26. Eskinazi, S., and W. Kruka, "Mixing of a Turbulent Wall Jet into a Free Stream," Transactions, American Society of Civil Engineers, Vol. 128, Part I, 1968, pp. 1055-1-073.
27. Pande, B.B.L., and N. Rajaratnam, "An Experimental Study of Bluff Buoyant Turbulent Surface Jets," Journal of Hydraulic Research, Vol. 15, No. 3, 1977, pp. 261-276.
28. Schwarz, W.H., and W.P. Cosart, "The Two-Dimensional Turbulent Wall Jet," Journal of Fluid Mechanics, Vol. 10, Part 4, June, 1961, pp. 481-495.

29. Stoy, R.L., M.H. Stenhouse, and A. Hsia, "Vortex Containment of Submerged Jet Discharge," Journal of the Hydraulics Division, American Society of Civil Engineers, Vol. 99, No. HY 9, Sept., 1973, pp. 1585-1598.
30. Hill, P.G., "Incompressible Jet Mixing in Coverging-Diverging Axisymmetric Ducts," Journal of Basic Engineering, Transactions of American Society of Mechanical Engineers, Vol. 89, Series D, No. 1, March, 1967, pp. 210-220.
31. Stoy, R.L., and Y. Ben-Haim, "Turbulent Jets in a Confined Cross-Flow," Journal of Fluids Engineering, Transactions of American Society of Mechanical Engineers, Vol. 95, Series 1, No. 4, Dec., 1973, pp. 551-556.
32. Sill, D.L., and J.A. Schetz, "Thermal Pollution in a Bounded Waterway," Thermal Pollution Analysis, American Institute of Aeronautics and Astronautics, 1974, pp. 121-138.
33. Sacks, S., J.E.A. John, and C.H. Marks, "Interaction of a Three-Dimensional Fluid Jet with a Nearby Wall Boundary," Thermal Pollution Analysis, American Institute of Aeronautics and Astronautics, 1974, pp. 259-280.
34. Wu, D., "Mathematical Modeling and Field Observations of Mixing Patterns from Waste Effluent Discharges," Ph.D. Dissertation, University of Wisconsin, Madison, 1974.
35. Shirazi, M.A., and L.R. Davis, "Workbook of Thermal Plume Prediction - Volume 2 - Surface Discharge," EPA-R2-72-005b, Environmental Protection Agency, May, 1974.
36. Lau, Y.L., "Temperature Distribution Due to the Release of Heated Effluents into Channel Flow," Technical Bulletin No. 55, Department of The Environment, Ottawa, Canada, 1971.
37. Sundaram, T.R., C.C. Easterbrook, K.R. Piech, and G. Rudinger, "An Investigation of the Physical Effects of Thermal Discharges into Cayuga Lake," Report No. VT-2616-02, Cornell Aeronautical Laboratory, Buffalo, New York, Nov., 1969.
38. Yotsukura, N., and E.D. Cobb, "Transverse Diffusion of Solutes in Natural Streams," U.S. Geological Survey Professional paper 582-C, 1972, 20 pp.
39. Yotsukura, N., and W.W. Sayre, "Transverse Mixing in Natural Channels," Water Resources Research, Vol. 12, No. 4, August, 1976, pp. 695-704.
40. Sium, O., "Transverse Flow Distribution in Natural Streams as Influenced by Cross-Sectional Shape," M.S. Thesis, Mechanics and Hydraulics Program, University of Iowa, 1975.
41. Bauer, D.P., H.E. Jobson, and M.E. Jennings, "Generalized Stream Temperature Analysis System," Hydraulic Engineering and the Environment, American Society of Civil Engineers, August, 1973, pp. 167-177.

42. Prakash, A., "Convective-Dispersion in Perennial Streams," Journal of the Environmental Engineering Division, American Society of Civil Engineers, Vol. 103, No. EE2, April 1977, pp. 321-340.
43. Benedict, B.A., Discussion of "Convective-Dispersion in Perennial Streams," Journal of the Environmental Engineering Division, ASCE, April, 1978, pp. 378-380.
44. Albertson, M.L., Y.B. Dai, R.A. Jensen, and H. Rouse, "Diffusion of Submerged Jets," Transactions, American Society of Civil Engineers, Vol. 115, pp. 639-664.
45. Stefan, H., and C. Shanmugham, "Flow Establishment and Initial Dilution of Heated Water Surface Jets," Proceedings, 17th Congress, International Association for Hydraulic Research, Baden-Baden, Germany.
46. Stefan, H.L., Bergstedt, and E. Mroska, "Flow Establishment and Initial Entrainment of Heated Water Surface Jets," U.S. Environmental Protection Agency, Ecological Research Series, No. EPA-660.3-75-014, May, 1975.
47. Brooks, N.H., "Diffusion of Sewage Effluent in an Ocean Current," Proceedings, First International Conference on Waste Disposal in the Marine Environment, Pergamon Press, 1960.
48. Holley, E.R., "Transverse Mixing In Rivers, Report Part I, Delft Hydraulics Laboratory, Report S132, Delft, The Netherlands, Dec., 1971.

APPENDIX

COMPUTER SOLUTION NOTES  
AND PROGRAM LISTING WITH EXAMPLE OUTPUT

## SUBROUTINE DESCRIPTIONS

### MAIN

This program merely controls the operation of the system. Data is read in by MAIN and then reported back to provide a record of the run. Then, the fourth-order Runge-Kutta routine, DRKGS, is called to provide the solution to the system of equations.

### DRKGS

This subroutine is from the IBM Scientific Subroutine Package and provides a fourth-order Runge-Kutta solution to a set of simultaneous differential equations. The integration increment, desired level of accuracy, and starting and ending points of the integration are specified by the user through input data cards. The user must write two subroutines, FCT and OUTP, for use with DRKGS, which calls both of them.

### FCT

This subroutine has the function of providing the current values of derivatives appearing on the left hand side of the NDIM simultaneous equations. (Here, NDIM=7 now.) Appendix A lists the non-dimensional equation forms. As can be seen there, in order to evaluate the derivatives at any location, it is first necessary to calculate current values for jet angle, dimensionless width, dimensionless velocity, and dimensionless DO and BOD values. These steps are carried out in FCT and then the values of the derivatives are calculated and stored as DERY (I) for return to DRKGS. The steps in solution of the equations for current parameter values are outlined in another segment of this appendix.

### OUTP

This subroutine checks for whether or not to output the current values of the parameters. If it is not desired to do so, then the subroutine merely returns control to DRKGS. If output is desired, then OUTP must solve for current values of the parameters using the same steps employed by FCT. Currently the subroutine is designed to output at selected increments of S, the dimensionless axial distance, as follows:

- for S = 0.0-1.0, output every 0.1
- for S = 1.0-100.0, output every 1.0
- for S = 100.0-SMAX, output every 10.0

OUTP functions on a line-by-line basis with no storage of values. However, it would be easy to store values for latter output or manipulation.

INPUT DATA SETUP  
FOR EXAMPLE RUN

---

---

0.0	100.0	0.10	1.D-5			
1.0	0.0	1.0	1.0	1.0	0.0	0.0
7						
0.0	0.0	0.0	0.0			
0.500	50.0	2.5	1.925D-3	0.639D-2		0.0D-0
1.2	16.27	0.416	1.38			
200.0	0.0	0.0	0.0	0.295		

---

---



the 1990s, the number of people in the United States who are 65 years of age or older has increased by 50 percent. The number of people 75 years of age or older has increased by 100 percent. The number of people 85 years of age or older has increased by 200 percent. The number of people 95 years of age or older has increased by 400 percent. The number of people 100 years of age or older has increased by 800 percent. The number of people 105 years of age or older has increased by 1,600 percent. The number of people 110 years of age or older has increased by 3,200 percent. The number of people 115 years of age or older has increased by 6,400 percent. The number of people 120 years of age or older has increased by 12,800 percent. The number of people 125 years of age or older has increased by 25,600 percent. The number of people 130 years of age or older has increased by 51,200 percent. The number of people 135 years of age or older has increased by 102,400 percent. The number of people 140 years of age or older has increased by 204,800 percent. The number of people 145 years of age or older has increased by 409,600 percent. The number of people 150 years of age or older has increased by 819,200 percent. The number of people 155 years of age or older has increased by 1,638,400 percent. The number of people 160 years of age or older has increased by 3,276,800 percent. The number of people 165 years of age or older has increased by 6,553,600 percent. The number of people 170 years of age or older has increased by 13,107,200 percent. The number of people 175 years of age or older has increased by 26,214,400 percent. The number of people 180 years of age or older has increased by 52,428,800 percent. The number of people 185 years of age or older has increased by 104,857,600 percent. The number of people 190 years of age or older has increased by 209,715,200 percent. The number of people 195 years of age or older has increased by 419,430,400 percent. The number of people 200 years of age or older has increased by 838,860,800 percent. The number of people 205 years of age or older has increased by 1,677,721,600 percent. The number of people 210 years of age or older has increased by 3,355,443,200 percent. The number of people 215 years of age or older has increased by 6,710,886,400 percent. The number of people 220 years of age or older has increased by 13,421,772,800 percent. The number of people 225 years of age or older has increased by 26,843,545,600 percent. The number of people 230 years of age or older has increased by 53,687,091,200 percent. The number of people 235 years of age or older has increased by 107,374,182,400 percent. The number of people 240 years of age or older has increased by 214,748,364,800 percent. The number of people 245 years of age or older has increased by 429,496,729,600 percent. The number of people 250 years of age or older has increased by 858,993,459,200 percent. The number of people 255 years of age or older has increased by 1,717,986,918,400 percent. The number of people 260 years of age or older has increased by 3,435,973,836,800 percent. The number of people 265 years of age or older has increased by 6,871,947,673,600 percent. The number of people 270 years of age or older has increased by 13,743,895,347,200 percent. The number of people 275 years of age or older has increased by 27,487,790,694,400 percent. The number of people 280 years of age or older has increased by 54,975,581,388,800 percent. The number of people 285 years of age or older has increased by 109,951,162,777,600 percent. The number of people 290 years of age or older has increased by 219,902,325,555,200 percent. The number of people 295 years of age or older has increased by 439,804,651,110,400 percent. The number of people 300 years of age or older has increased by 879,609,302,220,800 percent. The number of people 305 years of age or older has increased by 1,759,218,604,441,600 percent. The number of people 310 years of age or older has increased by 3,518,437,208,883,200 percent. The number of people 315 years of age or older has increased by 7,036,874,417,766,400 percent. The number of people 320 years of age or older has increased by 14,073,748,835,532,800 percent. The number of people 325 years of age or older has increased by 28,147,497,671,065,600 percent. The number of people 330 years of age or older has increased by 56,294,995,342,131,200 percent. The number of people 335 years of age or older has increased by 112,589,990,684,262,400 percent. The number of people 340 years of age or older has increased by 225,179,981,368,524,800 percent. The number of people 345 years of age or older has increased by 450,359,962,737,049,600 percent. The number of people 350 years of age or older has increased by 900,719,925,474,099,200 percent. The number of people 355 years of age or older has increased by 1,801,439,850,948,198,400 percent. The number of people 360 years of age or older has increased by 3,602,879,701,896,396,800 percent. The number of people 365 years of age or older has increased by 7,205,759,403,792,793,600 percent. The number of people 370 years of age or older has increased by 14,411,518,807,585,587,200 percent. The number of people 375 years of age or older has increased by 28,823,037,615,171,174,400 percent. The number of people 380 years of age or older has increased by 57,646,075,230,342,348,800 percent. The number of people 385 years of age or older has increased by 115,292,150,460,684,697,600 percent. The number of people 390 years of age or older has increased by 230,584,300,921,369,395,200 percent. The number of people 395 years of age or older has increased by 461,168,601,842,738,790,400 percent. The number of people 400 years of age or older has increased by 922,337,203,685,477,580,800 percent. The number of people 405 years of age or older has increased by 1,844,674,407,370,955,161,600 percent. The number of people 410 years of age or older has increased by 3,689,348,814,741,910,323,200 percent. The number of people 415 years of age or older has increased by 7,378,697,629,483,820,646,400 percent. The number of people 420 years of age or older has increased by 14,757,395,258,967,641,292,800 percent. The number of people 425 years of age or older has increased by 29,514,790,517,935,282,585,600 percent. The number of people 430 years of age or older has increased by 59,029,581,035,870,565,171,200 percent. The number of people 435 years of age or older has increased by 118,059,162,071,741,130,342,400 percent. The number of people 440 years of age or older has increased by 236,118,324,143,482,260,684,800 percent. The number of people 445 years of age or older has increased by 472,236,648,286,964,521,369,600 percent. The number of people 450 years of age or older has increased by 944,473,296,573,929,042,739,200 percent. The number of people 455 years of age or older has increased by 1,888,946,593,147,858,085,478,400 percent. The number of people 460 years of age or older has increased by 3,777,893,186,295,716,170,956,800 percent. The number of people 465 years of age or older has increased by 7,555,786,372,591,432,341,913,600 percent. The number of people 470 years of age or older has increased by 15,111,572,745,182,864,683,827,200 percent. The number of people 475 years of age or older has increased by 30,223,145,490,365,729,367,654,400 percent. The number of people 480 years of age or older has increased by 60,446,290,980,731,458,735,308,800 percent. The number of people 485 years of age or older has increased by 120,892,581,961,462,917,470,617,600 percent. The number of people 490 years of age or older has increased by 241,785,163,922,925,834,941,235,200 percent. The number of people 495 years of age or older has increased by 483,570,327,845,851,669,882,470,400 percent. The number of people 500 years of age or older has increased by 967,140,655,691,703,339,764,940,800 percent. The number of people 505 years of age or older has increased by 1,934,281,311,383,406,679,529,881,600 percent. The number of people 510 years of age or older has increased by 3,868,562,622,766,813,359,059,763,200 percent. The number of people 515 years of age or older has increased by 7,737,125,245,533,626,718,119,526,400 percent. The number of people 520 years of age or older has increased by 15,474,250,491,067,253,436,239,052,800 percent. The number of people 525 years of age or older has increased by 30,948,500,982,134,506,872,478,105,600 percent. The number of people 530 years of age or older has increased by 61,897,001,964,269,013,744,956,211,200 percent. The number of people 535 years of age or older has increased by 123,794,003,928,538,027,489,912,422,400 percent. The number of people 540 years of age or older has increased by 247,588,007,857,076,054,979,824,844,800 percent. The number of people 545 years of age or older has increased by 495,176,015,714,152,109,959,649,689,600 percent. The number of people 550 years of age or older has increased by 990,352,031,428,304,219,919,299,379,200 percent. The number of people 555 years of age or older has increased by 1,980,704,062,856,608,439,838,598,758,400 percent. The number of people 560 years of age or older has increased by 3,961,408,125,713,216,879,677,197,516,800 percent. The number of people 565 years of age or older has increased by 7,922,816,251,426,433,759,354,395,033,600 percent. The number of people 570 years of age or older has increased by 15,845,632,502,852,867,518,708,790,067,200 percent. The number of people 575 years of age or older has increased by 31,691,265,005,705

[illegible][illegible]

$\mathcal{C} = \{C_1, \dots, C_n\}$  is a  $\mathcal{C}$ -partition of  $\mathcal{A}$  if and only if  $\mathcal{C}$  is a partition of  $\mathcal{A}$  and  $\mathcal{C} \in \mathcal{C}$ .

[illegible]

$\mathcal{C} = \{C_1, C_2, \dots, C_n\}$ ,  $\mathcal{C} \subseteq \mathcal{C}'$ ,  $\mathcal{C}' = \{C'_1, C'_2, \dots, C'_m\}$ ,  $\mathcal{C} \cap \mathcal{C}' = \emptyset$ ,  $\mathcal{C} \cup \mathcal{C}' = \mathcal{C}''$ ,  $\mathcal{C}'' = \{C''_1, C''_2, \dots, C''_k\}$ ,  $\mathcal{C}'' \subseteq \mathcal{C}'''$ ,  $\mathcal{C}''' = \{C'''_1, C'''_2, \dots, C'''_l\}$ ,  $\mathcal{C}''' \subseteq \mathcal{C}^{(4)}$ ,  $\mathcal{C}^{(4)} = \{C^{(4)}_1, C^{(4)}_2, \dots, C^{(4)}_p\}$ ,  $\mathcal{C}^{(4)} \subseteq \mathcal{C}^{(5)}$ ,  $\mathcal{C}^{(5)} = \{C^{(5)}_1, C^{(5)}_2, \dots, C^{(5)}_q\}$ ,  $\mathcal{C}^{(5)} \subseteq \mathcal{C}^{(6)}$ ,  $\mathcal{C}^{(6)} = \{C^{(6)}_1, C^{(6)}_2, \dots, C^{(6)}_r\}$ ,  $\mathcal{C}^{(6)} \subseteq \mathcal{C}^{(7)}$ ,  $\mathcal{C}^{(7)} = \{C^{(7)}_1, C^{(7)}_2, \dots, C^{(7)}_s\}$ ,  $\mathcal{C}^{(7)} \subseteq \mathcal{C}^{(8)}$ ,  $\mathcal{C}^{(8)} = \{C^{(8)}_1, C^{(8)}_2, \dots, C^{(8)}_t\}$ ,  $\mathcal{C}^{(8)} \subseteq \mathcal{C}^{(9)}$ ,  $\mathcal{C}^{(9)} = \{C^{(9)}_1, C^{(9)}_2, \dots, C^{(9)}_u\}$ ,  $\mathcal{C}^{(9)} \subseteq \mathcal{C}^{(10)}$ ,  $\mathcal{C}^{(10)} = \{C^{(10)}_1, C^{(10)}_2, \dots, C^{(10)}_v\}$ ,  $\mathcal{C}^{(10)} \subseteq \mathcal{C}^{(11)}$ ,  $\mathcal{C}^{(11)} = \{C^{(11)}_1, C^{(11)}_2, \dots, C^{(11)}_w\}$ ,  $\mathcal{C}^{(11)} \subseteq \mathcal{C}^{(12)}$ ,  $\mathcal{C}^{(12)} = \{C^{(12)}_1, C^{(12)}_2, \dots, C^{(12)}_x\}$ ,  $\mathcal{C}^{(12)} \subseteq \mathcal{C}^{(13)}$ ,  $\mathcal{C}^{(13)} = \{C^{(13)}_1, C^{(13)}_2, \dots, C^{(13)}_y\}$ ,  $\mathcal{C}^{(13)} \subseteq \mathcal{C}^{(14)}$ ,  $\mathcal{C}^{(14)} = \{C^{(14)}_1, C^{(14)}_2, \dots, C^{(14)}_z\}$ ,  $\mathcal{C}^{(14)} \subseteq \mathcal{C}^{(15)}$ ,  $\mathcal{C}^{(15)} = \{C^{(15)}_1, C^{(15)}_2, \dots, C^{(15)}_a\}$ ,  $\mathcal{C}^{(15)} \subseteq \mathcal{C}^{(16)}$ ,  $\mathcal{C}^{(16)} = \{C^{(16)}_1, C^{(16)}_2, \dots, C^{(16)}_b\}$ ,  $\mathcal{C}^{(16)} \subseteq \mathcal{C}^{(17)}$ ,  $\mathcal{C}^{(17)} = \{C^{(17)}_1, C^{(17)}_2, \dots, C^{(17)}_c\}$ ,  $\mathcal{C}^{(17)} \subseteq \mathcal{C}^{(18)}$ ,  $\mathcal{C}^{(18)} = \{C^{(18)}_1, C^{(18)}_2, \dots, C^{(18)}_d\}$ ,  $\mathcal{C}^{(18)} \subseteq \mathcal{C}^{(19)}$ ,  $\mathcal{C}^{(19)} = \{C^{(19)}_1, C^{(19)}_2, \dots, C^{(19)}_e\}$ ,  $\mathcal{C}^{(19)} \subseteq \mathcal{C}^{(20)}$ ,  $\mathcal{C}^{(20)} = \{C^{(20)}_1, C^{(20)}_2, \dots, C^{(20)}_f\}$ ,  $\mathcal{C}^{(20)} \subseteq \mathcal{C}^{(21)}$ ,  $\mathcal{C}^{(21)} = \{C^{(21)}_1, C^{(21)}_2, \dots, C^{(21)}_g\}$ ,  $\mathcal{C}^{(21)} \subseteq \mathcal{C}^{(22)}$ ,  $\mathcal{C}^{(22)} = \{C^{(22)}_1, C^{(22)}_2, \dots, C^{(22)}_h\}$ ,  $\mathcal{C}^{(22)} \subseteq \mathcal{C}^{(23)}$ ,  $\mathcal{C}^{(23)} = \{C^{(23)}_1, C^{(23)}_2, \dots, C^{(23)}_i\}$ ,  $\mathcal{C}^{(23)} \subseteq \mathcal{C}^{(24)}$ ,  $\mathcal{C}^{(24)} = \{C^{(24)}_1, C^{(24)}_2, \dots, C^{(24)}_j\}$ ,  $\mathcal{C}^{(24)} \subseteq \mathcal{C}^{(25)}$ ,  $\mathcal{C}^{(25)} = \{C^{(25)}_1, C^{(25)}_2, \dots, C^{(25)}_k\}$ ,  $\mathcal{C}^{(25)} \subseteq \mathcal{C}^{(26)}$ ,  $\mathcal{C}^{(26)} = \{C^{(26)}_1, C^{(26)}_2, \dots, C^{(26)}_l\}$ ,  $\mathcal{C}^{(26)} \subseteq \mathcal{C}^{(27)}$ ,  $\mathcal{C}^{(27)} = \{C^{(27)}_1, C^{(27)}_2, \dots, C^{(27)}_m\}$ ,  $\mathcal{C}^{(27)} \subseteq \mathcal{C}^{(28)}$ ,  $\mathcal{C}^{(28)} = \{C^{(28)}_1, C^{(28)}_2, \dots, C^{(28)}_n\}$ ,  $\mathcal{C}^{(28)} \subseteq \mathcal{C}^{(29)}$ ,  $\mathcal{C}^{(29)} = \{C^{(29)}_1, C^{(29)}_2, \dots, C^{(29)}_o\}$ ,  $\mathcal{C}^{(29)} \subseteq \mathcal{C}^{(30)}$ ,  $\mathcal{C}^{(30)} = \{C^{(30)}_1, C^{(30)}_2, \dots, C^{(30)}_p\}$ ,  $\mathcal{C}^{(30)} \subseteq \mathcal{C}^{(31)}$ ,  $\mathcal{C}^{(31)} = \{C^{(31)}_1, C^{(31)}_2, \dots, C^{(31)}_q\}$ ,  $\mathcal{C}^{(31)} \subseteq \mathcal{C}^{(32)}$ ,  $\mathcal{C}^{(32)} = \{C^{(32)}_1, C^{(32)}_2, \dots, C^{(32)}_r\}$ ,  $\mathcal{C}^{(32)} \subseteq \mathcal{C}^{(33)}$ ,  $\mathcal{C}^{(33)} = \{C^{(33)}_1, C^{(33)}_2, \dots, C^{(33)}_s\}$ ,  $\mathcal{C}^{(33)} \subseteq \mathcal{C}^{(34)}$ ,  $\mathcal{C}^{(34)} = \{C^{(34)}_1, C^{(34)}_2, \dots, C^{(34)}_t\}$ ,  $\mathcal{C}^{(34)} \subseteq \mathcal{C}^{(35)}$ ,  $\mathcal{C}^{(35)} = \{C^{(35)}_1, C^{(35)}_2, \dots, C^{(35)}_u\}$ ,  $\mathcal{C}^{(35)} \subseteq \mathcal{C}^{(36)}$ ,  $\mathcal{C}^{(36)} = \{C^{(36)}_1, C^{(36)}_2, \dots, C^{(36)}_v\}$ ,  $\mathcal{C}^{(36)} \subseteq \mathcal{C}^{(37)}$ ,  $\mathcal{C}^{(37)} = \{C^{(37)}_1, C^{(37)}_2, \dots, C^{(37)}_w\}$ ,  $\mathcal{C}^{(37)} \subseteq \mathcal{C}^{(38)}$ ,  $\mathcal{C}^{(38)} = \{C^{(38)}_1, C^{(38)}_2, \dots, C^{(38)}_x\}$ ,  $\mathcal{C}^{(38)} \subseteq \mathcal{C}^{(39)}$ ,  $\mathcal{C}^{(39)} = \{C^{(39)}_1, C^{(39)}_2, \dots, C^{(39)}_y\}$ ,  $\mathcal{C}^{(39)} \subseteq \mathcal{C}^{(40)}$ ,  $\mathcal{C}^{(40)} = \{C^{(40)}_1, C^{(40)}_2, \dots, C^{(40)}_z\}$ ,  $\mathcal{C}^{(40)} \subseteq \mathcal{C}^{(41)}$ ,  $\mathcal{C}^{(41)} = \{C^{(41)}_1, C^{(41)}_2, \dots, C^{(41)}_a\}$ ,  $\mathcal{C}^{(41)} \subseteq \mathcal{C}^{(42)}$ ,  $\mathcal{C}^{(42)} = \{C^{(42)}_1, C^{(42)}_2, \dots, C^{(42)}_b\}$ ,  $\mathcal{C}^{(42)} \subseteq \mathcal{C}^{(43)}$ ,  $\mathcal{C}^{(43)} = \{C^{(43)}_1, C^{(43)}_2, \dots, C^{(43)}_c\}$ ,  $\mathcal{C}^{(43)} \subseteq \mathcal{C}^{(44)}$ ,  $\mathcal{C}^{(44)} = \{C^{(44)}_1, C^{(44)}_2, \dots, C^{(44)}_d\}$ ,  $\mathcal{C}^{(44)} \subseteq \mathcal{C}^{(45)}$ ,  $\mathcal{C}^{(45)} = \{C^{(45)}_1, C^{(45)}_2, \dots, C^{(45)}_e\}$ ,  $\mathcal{C}^{(45)} \subseteq \mathcal{C}^{(46)}$ ,  $\mathcal{C}^{(46)} = \{C^{(46)}_1, C^{(46)}_2, \dots, C^{(46)}_f\}$ ,  $\mathcal{C}^{(46)} \subseteq \mathcal{C}^{(47)}$ ,  $\mathcal{C}^{(47)} = \{C^{(47)}_1, C^{(47)}_2, \dots, C^{(47)}_g\}$ ,  $\mathcal{C}^{(47)} \subseteq \mathcal{C}^{(48)}$ ,  $\mathcal{C}^{(48)} = \{C^{(48)}_1, C^{(48)}_2, \dots, C^{(48)}_h\}$ ,  $\mathcal{C}^{(48)} \subseteq \mathcal{C}^{(49)}$ ,  $\mathcal{C}^{(49)} = \{C^{(49)}_1, C^{(49)}_2, \dots, C^{(49)}_i\}$ ,  $\mathcal{C}^{(49)} \subseteq \mathcal{C}^{(50)}$ ,  $\mathcal{C}^{(50)} = \{C^{(50)}_1, C^{(50)}_2, \dots, C^{(50)}_j\}$ ,  $\mathcal{C}^{(50)} \subseteq \mathcal{C}^{(51)}$ ,  $\mathcal{C}^{(51)} = \{C^{(51)}_1, C^{(51)}_2, \dots, C^{(51)}_k\}$ ,  $\mathcal{C}^{(51)} \subseteq \mathcal{C}^{(52)}$ ,  $\mathcal{C}^{(52)} = \{C^{(52)}_1, C^{(52)}_2, \dots, C^{(52)}_l\}$ ,  $\mathcal{C}^{(52)} \subseteq \mathcal{C}^{(53)}$ ,  $\mathcal{C}^{(53)} = \{C^{(53)}_1, C^{(53)}_2, \dots, C^{(53)}_m\}$ ,  $\mathcal{C}^{(53)} \subseteq \mathcal{C}^{(54)}$ ,  $\mathcal{C}^{(54)} = \{C^{(54)}_1, C^{(54)}_2, \dots, C^{(54$

[illegible]



[illegible]

[illegible]



[illegible]

```

247 10 CALL SUBROUTINE (X,Y,Z)
248 11 RETURN
249 12 END SUBROUTINE
250 20 IF (X=0) GO TO 2
251 21 IF (X=1) GO TO 3
252 22 IF (X=2) GO TO 4
253 23 IF (X=3) GO TO 5
254 24 IF (X=4) GO TO 6
255 25 IF (X=5) GO TO 7
256 26 IF (X=6) GO TO 8
257 27 IF (X=7) GO TO 9
258 28 IF (X=8) GO TO 10
259 29 IF (X=9) GO TO 11
260 30 IF (X=10) GO TO 12
261 31 IF (X=11) GO TO 13
262 32 IF (X=12) GO TO 14
263 33 IF (X=13) GO TO 15
264 34 IF (X=14) GO TO 16
265 35 IF (X=15) GO TO 17
266 36 IF (X=16) GO TO 18
267 37 IF (X=17) GO TO 19
268 38 IF (X=18) GO TO 20
269 39 IF (X=19) GO TO 21
270 40 IF (X=20) GO TO 22
271 41 IF (X=21) GO TO 23
272 42 IF (X=22) GO TO 24
273 43 IF (X=23) GO TO 25
274 44 IF (X=24) GO TO 26
275 45 IF (X=25) GO TO 27
276 46 IF (X=26) GO TO 28
277 47 IF (X=27) GO TO 29
278 48 IF (X=28) GO TO 30
279 49 IF (X=29) GO TO 31
280 50 IF (X=30) GO TO 32
281 51 IF (X=31) GO TO 33
282 52 IF (X=32) GO TO 34
283 53 IF (X=33) GO TO 35
284 54 IF (X=34) GO TO 36
285 55 IF (X=35) GO TO 37
286 56 IF (X=36) GO TO 38
287 57 IF (X=37) GO TO 39
288 58 IF (X=38) GO TO 40
289 59 IF (X=39) GO TO 41
290 60 IF (X=40) GO TO 42
291 61 IF (X=41) GO TO 43
292 62 IF (X=42) GO TO 44
293 63 IF (X=43) GO TO 45
294 64 IF (X=44) GO TO 46
295 65 IF (X=45) GO TO 47
296 66 IF (X=46) GO TO 48
297 67 IF (X=47) GO TO 49
298 68 IF (X=48) GO TO 50
299 69 IF (X=49) GO TO 51
300 70 IF (X=50) GO TO 52
301 71 IF (X=51) GO TO 53
302 72 IF (X=52) GO TO 54
303 73 IF (X=53) GO TO 55
304 74 IF (X=54) GO TO 56
305 75 IF (X=55) GO TO 57
306 76 IF (X=56) GO TO 58
307 77 IF (X=57) GO TO 59
308 78 IF (X=58) GO TO 60
309 79 IF (X=59) GO TO 61
310 80 IF (X=60) GO TO 62
311 81 IF (X=61) GO TO 63
312 82 IF (X=62) GO TO 64
313 83 IF (X=63) GO TO 65
314 84 IF (X=64) GO TO 66
315 85 IF (X=65) GO TO 67
316 86 IF (X=66) GO TO 68
317 87 IF (X=67) GO TO 69
318 88 IF (X=68) GO TO 70
319 89 IF (X=69) GO TO 71
320 90 IF (X=70) GO TO 72
321 91 IF (X=71) GO TO 73
322 92 IF (X=72) GO TO 74
323 93 IF (X=73) GO TO 75
324 94 IF (X=74) GO TO 76
325 95 IF (X=75) GO TO 77
326 96 IF (X=76) GO TO 78
327 97 IF (X=77) GO TO 79
328 98 IF (X=78) GO TO 80
329 99 IF (X=79) GO TO 81
330 100 IF (X=80) GO TO 82
331 101 IF (X=81) GO TO 83
332 102 IF (X=82) GO TO 84
333 103 IF (X=83) GO TO 85
334 104 IF (X=84) GO TO 86
335 105 IF (X=85) GO TO 87
336 106 IF (X=86) GO TO 88
337 107 IF (X=87) GO TO 89
338 108 IF (X=88) GO TO 90
339 109 IF (X=89) GO TO 91
340 110 IF (X=90) GO TO 92
341 111 IF (X=91) GO TO 93
342 112 IF (X=92) GO TO 94
343 113 IF (X=93) GO TO 95
344 114 IF (X=94) GO TO 96
345 115 IF (X=95) GO TO 97
346 116 IF (X=96) GO TO 98
347 117 IF (X=97) GO TO 99
348 118 IF (X=98) GO TO 100
349 119 IF (X=99) GO TO 101
350 120 IF (X=100) GO TO 102
351 121 IF (X=101) GO TO 103
352 122 IF (X=102) GO TO 104
353 123 IF (X=103) GO TO 105
354 124 IF (X=104) GO TO 106
355 125 IF (X=105) GO TO 107
356 126 IF (X=106) GO TO 108
357 127 IF (X=107) GO TO 109
358 128 IF (X=108) GO TO 110
359 129 IF (X=109) GO TO 111
360 130 IF (X=110) GO TO 112
361 131 IF (X=111) GO TO 113
362 132 IF (X=112) GO TO 114
363 133 IF (X=113) GO TO 115
364 134 IF (X=114) GO TO 116
365 135 IF (X=115) GO TO 117
366 136 IF (X=116) GO TO 118
367 137 IF (X=117) GO TO 119
368 138 IF (X=118) GO TO 120
369 139 IF (X=119) GO TO 121
370 140 IF (X=120) GO TO 122
371 141 IF (X=121) GO TO 123
372 142 IF (X=122) GO TO 124
373 143 IF (X=123) GO TO 125
374 144 IF (X=124) GO TO 126
375 145 IF (X=125) GO TO 127
376 146 IF (X=126) GO TO 128
377 147 IF (X=127) GO TO 129
378 148 IF (X=128) GO TO 130
379 149 IF (X=129) GO TO 131
380 150 IF (X=130) GO TO 132
381 151 IF (X=131) GO TO 133
382 152 IF (X=132) GO TO 134
383 153 IF (X=133) GO TO 135
384 154 IF (X=134) GO TO 136
385 155 IF (X=135) GO TO 137
386 156 IF (X=136) GO TO 138
387 157 IF (X=137) GO TO 139
388 158 IF (X=138) GO TO 140
389 159 IF (X=139) GO TO 141
390 160 IF (X=140) GO TO 142
391 161 IF (X=141) GO TO 143
392 162 IF (X=142) GO TO 144
393 163 IF (X=143) GO TO 145
394 164 IF (X=144) GO TO 146
395 165 IF (X=145) GO TO 147
396 166 IF (X=146) GO TO 148
397 167 IF (X=147) GO TO 149
398 168 IF (X=148) GO TO 150
399 169 IF (X=149) GO TO 151
400 170 IF (X=150) GO TO 152
401 171 IF (X=151) GO TO 153
402 172 IF (X=152) GO TO 154
403 173 IF (X=153) GO TO 155
404 174 IF (X=154) GO TO 156
405 175 IF (X=155) GO TO 157
406 176 IF (X=156) GO TO 158
407 177 IF (X=157) GO TO 159
408 178 IF (X=158) GO TO 160
409 179 IF (X=159) GO TO 161
410 180 IF (X=160) GO TO 162
411 181 IF (X=161) GO TO 163
412 182 IF (X=162) GO TO 164
413 183 IF (X=163) GO TO 165
414 184 IF (X=164) GO TO 166
415 185 IF (X=165) GO TO 167
416 186 IF (X=166) GO TO 168
417 187 IF (X=167) GO TO 169
418 188 IF (X=168) GO TO 170
419 189 IF (X=169) GO TO 171
420 190 IF (X=170) GO TO 172
421 191 IF (X=171) GO TO 173
422 192 IF (X=172) GO TO 174
423 193 IF (X=173) GO TO 175
424 194 IF (X=174) GO TO 176
425 195 IF (X=175) GO TO 177
426 196 IF (X=176) GO TO 178
427 197 IF (X=177) GO TO 179
428 198 IF (X=178) GO TO 180
429 199 IF (X=179) GO TO 181
430 200 IF (X=180) GO TO 182
431 201 IF (X=181) GO TO 183
432 202 IF (X=182) GO TO 184
433 203 IF (X=183) GO TO 185
434 204 IF (X=184) GO TO 186
435 205 IF (X=185) GO TO 187
436 206 IF (X=186) GO TO 188
437 207 IF (X=187) GO TO 189
438 208 IF (X=188) GO TO 190
439 209 IF (X=189) GO TO 191
440 210 IF (X=190) GO TO 192
441 211 IF (X=191) GO TO 193
442 212 IF (X=192) GO TO 194
443 213 IF (X=193) GO TO 195
444 214 IF (X=194) GO TO 196
445 215 IF (X=195) GO TO 197
446 216 IF (X=196) GO TO 198
447 217 IF (X=197) GO TO 19
```



294            30    10    2    .  
 295            37    10    1    2  
 296            40    10    1    2  
 297            38    10    1    2  
 298            39    10    1    2  
 299            40    10    1    2  
 300            40    10    1    2

SDATA

0.295

VELOCITY RATIO =  $U/V_{\infty}$  = .7  
 INITIAL ANGLE AT  $t = 0$  =  $20^\circ$  = .35  
 REDUCED DRAG COEFFICIENT =  $C_D/C_{D0}$  = 1.0  
 DIMENSIONLESS DEOXYGENATION COEFFICIENT =  $k_1/k_2$  = 1.0  
 DIMENSIONLESS REGENERATION COEFFICIENT =  $k_2/k_1$  = 1.0  
 DIMENSIONLESS SEDIMENTATION COEFFICIENT =  $k_3/k_1$  = 1.0  
 RATIO  $LAZ/D = C_L$  = .00000000  
 RATIO  $DAZ/D = C_{L2}$  = .00000000  
 RATIO  $BAZ/D = C_{L3}$  = .00000000  
 RATIO  $DOZ/D = C_{L4}$  = .00000000  
 INITIAL DISCHARGE COEFFICIENT =  $C_{D0}$  = 1.0  
 INITIAL DISCHARGE COEFFICIENT =  $C_{D1}$  = 1.0  
 DEOXYGENATION COEFFICIENT =  $k_1$  = 1.0  
 REGENERATION COEFFICIENT =  $k_2$  = 1.0  
 INITIAL  $PO_2$  = 200.0  
 INITIAL EFFICIENCY = .7  
 AMBIENT  $PO_2$  = .  
 AMBIENT EFFICIENCY = .

OUTPUT OF JET MODEL

S	X	Y	44 18	P/100	HC/100	L/10	XM	YB	W
0.00000	0.00000	0.00000	50.00000	1.00000	1.00000	1.00000	0.00000	0.00000	1.35721
0.10000	0.06000	0.07143	49.00000	1.00000	1.00000	0.99720	0.00120	0.00000	1.35721
0.20000	0.14000	0.13426	48.00000	1.00000	1.00000	0.99440	0.00260	0.00000	1.35721
0.30000	0.23000	0.19682	47.00000	1.00000	1.00000	0.99160	0.00400	0.00000	1.35721
0.40000	0.32000	0.25938	46.00000	1.00000	1.00000	0.98880	0.00540	0.00000	1.35721
0.50000	0.41000	0.32194	45.00000	1.00000	1.00000	0.98600	0.00680	0.00000	1.35721
0.60000	0.50000	0.38450	44.00000	1.00000	1.00000	0.98320	0.00820	0.00000	1.35721
0.70000	0.59000	0.44706	43.00000	1.00000	1.00000	0.98040	0.00960	0.00000	1.35721
0.80000	0.68000	0.50962	42.00000	1.00000	1.00000	0.97760	0.01100	0.00000	1.35721
0.90000	0.77000	0.57218	41.00000	1.00000	1.00000	0.97480	0.01240	0.00000	1.35721
1.00000	0.86000	0.63474	40.00000	1.00000	1.00000	0.97200	0.01380	0.00000	1.35721
2.00000	1.84000	0.53053	39.00000	1.00000	1.00000	0.96920	0.01520	0.00000	1.35721
3.00000	2.82000	0.42632	38.00000	1.00000	1.00000	0.96640	0.01660	0.00000	1.35721
4.00000	3.80000	0.32211	37.00000	1.00000	1.00000	0.96360	0.01800	0.00000	1.35721
5.00000	4.78000	0.21790	36.00000	1.00000	1.00000	0.96080	0.01940	0.00000	1.35721
6.00000	5.76000	0.11369	35.00000	1.00000	1.00000	0.95800	0.02080	0.00000	1.35721
7.00000	6.74000	0.00948	34.00000	1.00000	1.00000	0.95520	0.02220	0.00000	1.35721
8.00000	7.72000	0.00527	33.00000	1.00000	1.00000	0.95240	0.02360	0.00000	1.35721
9.00000	8.70000	0.00106	32.00000	1.00000	1.00000	0.94960	0.02500	0.00000	1.35721
10.00000	9.68000	0.00000	31.00000	1.00000	1.00000	0.94680	0.02640	0.00000	1.35721
11.00000	10.66000	0.00000	30.00000	1.00000	1.00000	0.94400	0.02780	0.00000	1.35721
12.00000	11.64000	0.00000	29.00000	1.00000	1.00000	0.94120	0.02920	0.00000	1.35721
13.00000	12.62000	0.00000	28.00000	1.00000	1.00000	0.93840	0.03060	0.00000	1.35721
14.00000	13.60000	0.00000	27.00000	1.00000	1.00000	0.93560	0.03200	0.00000	1.35721
15.00000	14.58000	0.00000	26.00000	1.00000	1.00000	0.93280	0.03340	0.00000	1.35721
16.00000	15.56000	0.00000	25.00000	1.00000	1.00000	0.93000	0.03480	0.00000	1.35721
17.00000	16.54000	0.00000	24.00000	1.00000	1.00000	0.92720	0.03620	0.00000	1.35721
18.00000	17.52000	0.00000	23.00000	1.00000	1.00000	0.92440	0.03760	0.00000	1.35721
19.00000	18.50000	0.00000	22.00000	1.00000	1.00000	0.92160	0.03900	0.00000	1.35721
20.00000	19.48000	0.00000	21.00000	1.00000	1.00000	0.91880	0.04040	0.00000	1.35721
21.00000	20.46000	0.00000	20.00000	1.00000	1.00000	0.91600	0.04180	0.00000	1.35721
22.00000	21.44000	0.00000	19.00000	1.00000	1.00000	0.91320	0.04320	0.00000	1.35721
23.00000	22.42000	0.00000	18.00000	1.00000	1.00000	0.91040	0.04460	0.00000	1.35721
24.00000	23.40000	0.00000	17.00000	1.00000	1.00000	0.90760	0.04600	0.00000	1.35721
25.00000	24.38000	0.00000	16.00000	1.00000	1.00000	0.90480	0.04740	0.00000	1.35721
26.00000	25.36000	0.00000	15.00000	1.00000	1.00000	0.90200	0.04880	0.00000	1.35721
27.00000	26.34000	0.00000	14.00000	1.00000	1.00000	0.89920	0.05020	0.00000	1.35721
28.00000	27.32000	0.00000	13.00000	1.00000	1.00000	0.89640	0.05160	0.00000	1.35721
29.00000	28.30000	0.00000	12.00000	1.00000	1.00000	0.89360	0.05300	0.00000	1.35721
30.00000	29.28000	0.00000	11.00000	1.00000	1.00000	0.89080	0.05440	0.00000	1.35721
31.00000	30.26000	0.00000	10.00000	1.00000	1.00000	0.88800	0.05580	0.00000	1.35721
32.00000	31.24000	0.00000	9.00000	1.00000	1.00000	0.88520	0.05720	0.00000	1.35721
33.00000	32.22000	0.00000	8.00000	1.00000	1.00000	0.88240	0.05860	0.00000	1.35721
34.00000	33.20000	0.00000	7.00000	1.00000	1.00000	0.87960	0.06000	0.00000	1.35721
35.00000	34.18000	0.00000	6.00000	1.00000	1.00000	0.87680	0.06140	0.00000	1.35721
36.00000	35.16000	0.00000	5.00000	1.00000	1.00000	0.87400	0.06280	0.00000	1.35721
37.00000	36.14000	0.00000	4.00000	1.00000	1.00000	0.87120	0.06420	0.00000	1.35721
38.00000	37.12000	0.00000	3.00000	1.00000	1.00000	0.86840	0.06560	0.00000	1.35721
39.00000	38.10000	0.00000	2.00000	1.00000	1.00000	0.86560	0.06700	0.00000	1.35721
40.00000	39.08000	0.00000	1.00000	1.00000	1.00000	0.86280	0.06840	0.00000	1.35721
41.00000	40.06000	0.00000	0.00000	1.00000	1.00000	0.86000	0.06980	0.00000	1.35721
42.00000	41.04000	0.00000	0.00000	1.00000	1.00000	0.85720	0.07120	0.00000	1.35721
43.00000	42.02000	0.00000	0.00000	1.00000	1.00000	0.85440	0.07260	0.00000	1.35721
44.00000	43.00000	0.00000	0.00000	1.00000	1.00000	0.85160	0.07400	0.00000	1.35721
45.00000	44.00000	0.00000	0.00000	1.00000	1.00000	0.84880	0.07540	0.00000	1.35721
46.00000	45.00000	0.00000	0.00000	1.00000	1.00000	0.84600	0.07680	0.00000	1.35721
47.00000	46.00000	0.00000	0.00000	1.00000	1.00000	0.84320	0.07820	0.00000	1.35721
48.00000	47.00000	0.00000	0.00000	1.00000	1.00000	0.84040	0.07960	0.00000	1.35721
49.00000	48.00000	0.00000	0.00000	1.00000	1.00000	0.83760	0.08100	0.00000	1.35721
50.00000	49.00000	0.00000	0.00000	1.00000	1.00000	0.83480	0.08240	0.00000	1.35721
51.00000	50.00000	0.00000	0.00000	1.00000	1.00000	0.83200	0.08380	0.00000	1.35721



END

FILMED

1-90

DTIC